University of Biskra
Faculty of Sciences and Technology
Department of Mechanical Engineering

MASTER THESIS

Domain: Sciences and Technology
Division: Mechanical Engineering
Specialty: Energetic

Ref.: .....

Prepared by:
Abdelhaie FETITI
Said BENCHAA

Rheological characterization of local agro-food products: Apricot jam flow behaviour

Jury:

Pr.	Noureddine MOUMMI	University of Biskra	President
Pr.	Adel BENCHABANE	University of Biskra	Supervisor
Dr.	Salah GUERBAAI	University of Biskra	Examiner

Academic year: 2021 – 2022

Acknowledgement

First, we thank Allah for everything and for enabling us to do this work, and we must thank our parents for their love and support throughout our lives. Thank you for giving us the strength to chase our dreams. Thanks to all of our families for their support. We thank all the professors who taught us from primary education to entering the university.

Thank you very much Prof. Adel Benchabane our supervisor. We would also like to thank Dr. Mohamed-Chaouki NEBBAR, head of the Technical Platform of Physicochemical Analyzes PTAPC - CRAPC - Biskra, as well as the engineers: Dr. Samir HAMEURLAINE, Dr. Karima LAMAMRA, Mr. Boualem DJRIDI and Ms Aida GHAZALI for their precious help to carrying out the experimental study.

We thank Prof. Noureddine MOUMMI, the jury president, and Dr. Salah GUERBAAI, the examiner of this work. We thank all the members of the university family, especially all the professors of mechanical engineering, whom we consider the best professors of the university. Thanks to all our friends, thank you for your understanding and encouragement in many moments.

Table of contents

List of figures

List of Table

Nomenclature

σ_E: Tensile stress (pa)

F: force shear rate (N)

σ: Shear stress (pa)

F_n: Normal force (N)

F_σ: Tangential forces (N)

τ: shear stress (pa)

$\dot{\gamma}$: Velocity gradient (m/s)

ω The speed of rotation (tr/min)

M: The torque imposed on the cone (N.m)

R: the radius of the cone (mm)

Ω : Rotor angular velocity (rad/s)

η_c : The corrected local viscosity (pa/s)

I: the moment of inertia of the mobile tool ($Kg.m^2$)

$\dot{\Omega}$: The angular acceleration of the rotor (rad/s^2)

Ψ:The angle of inclination (degree)

K : The constant relating to the cone-plane geometry (m^{-3}).

τ_c: corrected stress (pa).

η: Coefficient of viscosity (pa/s).

γ: shear strain (rad).

$\dot{\gamma}$: The shear rate (1/s)

A: the shear plane (m^2)

V: the velocity (m/s)

h: is the gap width (m)

B_{xy}: The shear strain (rad)

$2D_{xy}$: The shear rate (1/s)

T_{xy}: Shear stress (pa)

r_0: Radius of the outer cylinders (mm).

r_1: Radius of inner cylinders (mm).

C: the couple on the cylinders (N.m)

L: the effective immersed length (m)

Ω_1: The angular velocity of the inner (rad/s)

k_2: The consistency (pa.s^n)

n: the power-law index

b: the ratio of the inner.

τ_a: Newtonian shear stress (pa).

General introduction

Rheology, as an independent branch of physic, emerged more than 90 years ago. It originated from observations of “strange” or abnormal behaviour of many well-known materials and difficulties in answering some “simple” questions [1].

- Clays look solid but they can be moulded into a shape; they may occupy vessels the way any liquid does; why do clays behave like many liquids?
- yogurt does not flow out of a container (it has high viscosity), but after intensive mixing its viscosity decreases, and then increases again when left to rest, so which value of viscosity should be considered?
- Concrete mix appears to be solid and rigid, but when subjected to an external force it changes its shape similar to liquids; what are the reasons for such behaviour?
- parts made out of polymeric materials (plastics) look solid and hard, similar to parts made out of metal, but they are noticeably different: when force is applied to a metallic part it slightly changes its shape and maintains its new shape for a long time; this is not the case with plastics which also change their shape after force is applied but they continue to change shape; if this material is solid, why does it “creep”? [1].

Most people are familiar with the basics of rheology from experience. The word rheology was invented in 1929 to name the discipline of a society engaged in the study of how materials deform in response to forces. It was inspired by a quote by Heraclitus: “παντα ρει” translated as “everything flows”. Indeed, everything does flow, but to different extents depending on how much force is applied, in what direction, and for how long. For materials more complex than simple springs, where a spring constant relates force to elongation, the goal of rheology is to provide quantitative parameters that define how a material will deform as a function of force, time and spatial orientation [2].

Even when analysis equipment is available, quality control of the rheological behaviour of agro-food products remains a delicate task. This type of mechanical analysis requires know-how, particularly in the choice of measurement geometry, measurement protocols and results analysis.

This work is an experimental contribution to the study of rheology and fluid flow. The study concerns the discovery of the rheological properties of apricot jam using a Hybrid

rheometer (hr20). The manuscript is presented in four chapters: i) Rotational rheometry, ii) General description of the HR20, iii) Materials and methods and iv) Rheological characterization of apricot jam.

Chapter I: Rotational rheometry

I.1 Introduction

The practical use of rheology is presented in the following areas: quality control (QC), production and application, chemical and mechanical engineering, industrial research and development, and materials science.

The first computer-controlled rheometers came into use in industrial laboratories in the mid-1980s. Ever since then, test methods as well as control and analysis options have improved with breathtaking speed. In order to organize and clarify the growing mountain of information, company Anton Paar Germany – and previously Physical Messtechnik – has offered basic seminars on rheology already since 1988, focused on branch-specific industrial application [3].

I.2 Rheology

Rheology is the science of deformation and flow. It is a branch of physics (and physical chemistry) since the most important variables come from the field of mechanics: forces, deflections and velocities. The term "rheology" originates from the Greek: "rheos" meaning "the river", "flowing", "streaming". Thus, rheology is literally "flow science". However, rheological experiments do not merely reveal information about the flow behaviour of liquids, but also the deformation behaviour of solids. The connection here is that a large deformation produced by shear forces cause many materials to flow. All forms of shear behaviour, which can be described rheologically in a scientific way, can be viewed as being in between two extremes: the flow of ideal viscous liquids on one hand and the deformation of ideal elastic solids on the other. Two illustrative examples for the extremes of ideal behaviour are a low-viscosity mineral oil and a steel ball. The behaviour of all real materials is based on the combination of both the viscous and the elastic portion and therefore, it is called viscoelastic. Wallpaper paste is a viscoelastic liquid, for example, and a gum eraser is a viscoelastic solid [4].

liquid		solids	
(ideal)viscous Flow behaviour Newton's law	Viscoelastic Flow behaviour Maxwell's law	Viscoelastic Deformation behaviour Kelvin/voigt's law	(ideal) elastic Deformation behaviour Hooke's law
Flow/viscosity curves	Creep tests, relaxation test, oscillatory tests		

Table I-1: overview on different kinds of rheological behaviour

Rheology was first seen as a science in its own right not before the beginning of the 20th century. However, scientists have long before been interested in the behaviour of liquids and solids, although some of their methods have not always been very scientific. Of special interest are here the various attempts to classify all kinds of different rheological behaviour, such as the classification of Markus Reiner in 1931 and 1960, and of George W. Scott Blair in 1942. A rheologist aims to measure the flow and deformation behaviour, and to present and explain the results clearly [4].

I.3 Newtonian fluids

Ideal fluids (e.g. water, methanol, olive oil and glycerol) perform linearly in rheograms, and are identified as Newtonian fluids. The Newtonian equation (Eq. I-1) illustrates the flow behaviour of an ideal liquid where η is the viscosity (Pa*s). Dynamic viscosity, also called apparent viscosity, describes a fluid's resistance of deformation. In terms of rheology, it is the relation of shear stress over the shear rate (Eq. I-2). For Newtonian fluids, the dynamic viscosity maintains a constant value meaning a linear relationship between τ and$\dot{\gamma}$ [5].

$$\tau = \eta * \dot{\gamma} \qquad \text{I-1}$$

$$\eta = \tau/\dot{\gamma} \qquad \text{I-2}$$

When measuring the dynamic viscosity, the fluid is subjected to a force impact caused by moving a body in the fluid. Resistance to this movement provides a measure of fluid viscosity. The dynamic viscosity can be measured using a rotation rheometer. The device consists of an external fixed cylinder with known radius and an internal cylinder or spindle with known radius and height. The space between the two cylinders is filled with the fluid subjected to dynamic viscosity analysis [5].

I.4 Non-Newtonian

Non-Newtonian fluids do not show a linear relationship between shear stress and shear rate. This is due to the complex structure and deformation effects exhibited by the materials involved in such fluids. The non-Newtonian fluids are however diverse and can be characterised as e.g. pseudoplastic, viscoplastic, dilatant and thixotropic fluids [5].

I.5 Rheometry

Rheometry is the measuring technology used to determine rheological data. The emphasis here is on measuring systems, instruments, and test and analysis methods. Both, liquids and solids can be investigated using rotational and oscillatory rheometers [4].

I.6 STRESSES

Internal stresses are directly related to forces applied to a body regardless of their origin. Only in special cases do internal stresses exist in the absence of external forces. These are, for example, thermal stresses caused by temperature inhomogeneity throughout a body or frozen stresses stored as a result of thermal and/or mechanical history of a body treatment caused by its heterogeneity [1]

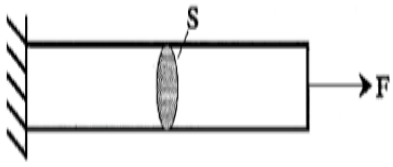

Figure I-1: A bar loaded with a normal force.

I.6.1 General theory

Any external force applied to a body leads either to a movement of the body as a whole or to a change of its initial shape. Both may occur simultaneously. The movement of a body in space and/or its rotation around its center of gravity, with no change to its shape is a subject of study by mechanics, and as such is not discussed in this book. The principal focus of our discussion here are changes which occur inside a body on application of an external force. The applied forces create dynamic reactions at any point of a body, which are characterized by a physical factor called stress [1].

Stress can be explained using a simple example. Let us consider a body (a bar). The area of its normal cross-section is S (Fig I-1). The force, F, is normal to the surface, S. The specific force at any point of the cross-section equals F/S. The ratio is a normal stress or a tensile stress, σ_E :

$$\sigma_E = \frac{F}{s} \qquad I\text{-}3$$

Stress is the force per unit of the surface area. The force at any surface may not be constant, i.e., be a function of coordinates. For example, a train moving on rails presses rails at local zones (where wheels touch the rail). The force is then distributed within the rail according to a complex pattern of stress distribution.

In our case, we do not consider force distribution because we have selected a small surface area, ΔS. A relative (specific) force, ΔF, acting on the area of ΔS is used to calculate the ratio ΔF/ΔS. By decreasing the surface area, we eventually come to its limiting form, as follows: [1]

$$\sigma = lim\frac{\Delta F}{\Delta s}\ at\ \Delta s \to 0, \sigma = \frac{dF}{ds} \qquad I\text{-}4$$

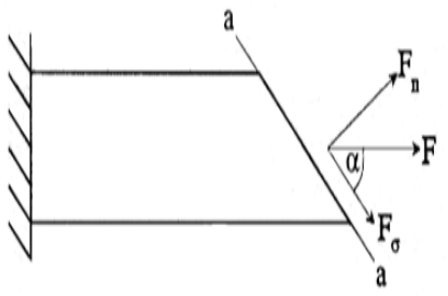

Figure I-2: Stresses on the inclined section of a bar − decomposition of a normal force at the arbitrary oriented surface.

I.6.2 PRINCIPAL STRESSES

The concept of principal stresses is a consequence of the dependence of stresses on the orientation of a surface. If stress components change on rotation of the coordinate axes, there must be such orientation of axes, at which the numerical values of these components are extreme (maximum or minimum) [1].

This idea is illustrated by a simple two-dimensional example generated from Fig I-1. Let the bar be cut at some angle α, as shown in Fig.I-2 , and let the force F act at this angle α to the plane aa. Then, it is easy to calculate two components of the vector F − normal and tangential forces, F_n and Fσ, respectively:

$$F_n = Fsin\alpha; F_\sigma = F = FcosF$$

Then, the stress tensor components can be found, taking into account that the surface area of the inclined cross-section is S/sinα. Stress components, related to the force per unit of surface area, are found as follows:

Normal stress, σ_E

$$\sigma_E = \frac{F_n}{S} sin\alpha = \frac{F}{S} sin^2\alpha = \sigma_0 sin^2\alpha \qquad \textit{I-5}$$

Shear stress, σ:

$$\sigma = \frac{F_\sigma}{S} sin\alpha = \frac{F}{S} sin\alpha\, cos\alpha = \frac{\sigma_0}{2} sin2\alpha \qquad \text{I-6}$$

Where σ_0=F/S.

The following special orientations can be found in a body:

At α = 90° the normal stress $\sigma_E = \sigma_0$ is at maximum, and the shear stress σ = 0;

At α = 45° the normal stress $\sigma_E = \sigma_0/2$and the shear stress $\sigma = \sigma_0$is at maximum;

At α = 0° both σ_E and σ are equal zero, this plane is free from stresses [1].

I.7 Techniques de measures rhéologiques

Rheological measurement techniques Using rheometers or viscometers, flows are produced which make it possible, on the basis of geometric considerations and hypotheses on the flow, to link the macroscopic parameters (torque, speed of rotation, flow rate, difference in pressure…) to the parameters governing the constitutive laws which are in general the shearing stress τ and the velocity gradient$\dot{\gamma}$.

The techniques that are often used are: I) Capillary, the principle of which is based on the flow in a cylindrical pipe. II) Rotating rheometers in which the fluid is sheared between two coaxial cylinders, between two planes or between a plane and a cone. These rheometers make it possible to determine the flow [$\tau = f(\dot{\gamma})$]and viscoelastic behaviour of the materials. In such tests, the sample is subjected to a constant or oscillatory stress (stress or shear applied depending on the type of rheometer). , and we study his answer in the moments that follow.

Note that capillary and rotational rheometers are not the only ones used. We cite for example Rheometry by MRI (magnetic resonance imaging) which is often encountered in recent literature. This technique is in full expansion. Indeed, it makes it possible to obtain local information without disturbances of the flow and no marker is necessary. Miller (1998) provides a non-exhaustive review of the various techniques used as well as possible applications, particularly in the rheology of fluids and granular materials. With regard to the techniques specific to nuclear magnetic resonance, specialized works provide more complete information

such as that of Callaghan (1991).It is noted that this technique made it possible to obtain information in very complex geometries [6].

I.7.1 Example of Measurement geometry

I.7.1.1 (Cone-plane geometry)

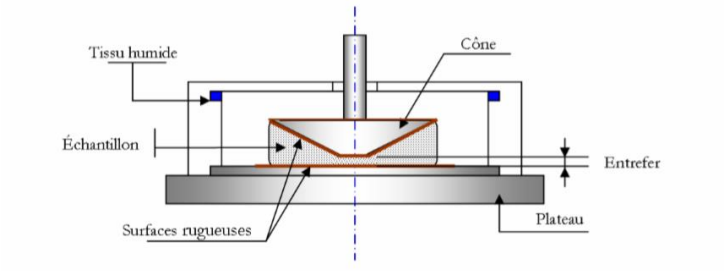

Figure I-3: cone-plane geometry

The principle of measurement for this geometry is simple. In fact, the rotation of the sample requires the conversion of rotational speed and torsion torque into speed and shear stress, according to the following two relationships:

$$\dot{\gamma} = \frac{1}{\delta}.\omega \qquad \text{I-7}$$

$$\tau = \frac{3}{2.\pi.R^3}.M \qquad \textit{I-8}$$

Where: δ is the angle of the cone, ω the speed of rotation of the cone or the plate, M the torque imposed on the cone and R the radius of the cone [6].

I.7.1.2 Parallel plate geometry

This geometry is composed of two coaxial discs in relative rotation (fig I-4). In general, the upper disc is mobile while the lower disc is fixed. The main advantage of this geometry is that the installation requires a small quantity of fluid to be measured and easy cleaning. In addition, the air gap (space between the two discs) of this geometry can be adjusted to the desired thickness. This therefore makes it possible to test materials containing particles of various sizes [7].

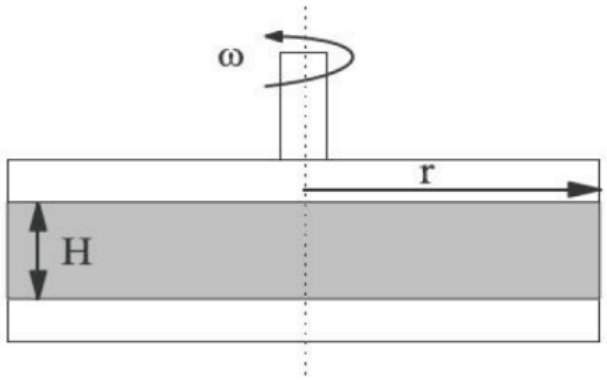

Figure I-4: Parallel plate geometry:

With this geometry, it is assumed that the flow is quasi-static. The velocity field in the fluid is written:

$$\underline{V} = \omega \frac{r\, z}{H} \underline{e}\theta \qquad \textit{I-9}$$

With:

$$\dot{\gamma}(r) = \omega \frac{r}{H} \qquad \textit{I-10}$$

$$\tau(\dot{\gamma}_R) = \frac{3C}{2\pi R^3} + \frac{\dot{\gamma}_R}{2\pi R^3} \frac{dc}{d\dot{\gamma}_R} \qquad \textit{I-11}$$

Where C designates the torque, ω the speed of rotation of the mobile disc, R the radius of the disc [7].

I.7.2 Evaporation problem

It intervenes especially in the suspensions during tests comprising a free surface. This phenomenon leads to a decrease in the volume studied. This could result in a decrease in the measured apparent viscosity. On the other hand, an increase in the mass concentration appears, which results in an increase in the apparent viscosity. The practical techniques, used to minimize the disturbances, consist in working under an atmosphere saturated by the interstitial fluid or in placing a liquid film on the free surfaces [6].

I.7.3 Slip at the walls

This is the most common phenomenon encountered during the rheological study of fluids. It can occur in all flow geometries and results from the preferential shearing of a thin layer of the fluid under test near the walls. This phenomenon leads to measurement errors, in particular for threshold stress measurements with an imposed stress rheometer [Barnes (1995); Bonifas (1998)]. In the case of suspensions, sliding can be favored by the migration of particles from the parietal regions (decrease in the solid concentration near the smooth wall), an effect known as the sigma effect. This effect has been addressed by many authors, such as Quemada, for example, who reported the existence of this phenomenon in cylindrical pipes [Quemada (1977); (1978a) and (1978b)]. Work on the rheometry of clay suspensions has also shown the existence of this phenomenon at the walls [Yoshimura and Prud'homme (1988)]. These authors developed a mathematical model inspired by that of Mooney (1931).

The method of Yoshimura and Prud'homme (1988) consists in carrying out two series of measurements on geometries of the same type but with a single different characteristic. In another work and as part of his thesis, Bonifas (1998) took up the calculation method of Yoshimura and Prud'homme (1988) on bentonite suspensions using plane-plane and plane-cone geometries. He concluded that this model achieves a non-negligible and acceptable correction.

On the other hand, and alongside these calculation methods, we note the existence of another method where the sliding effect is controlled experimentally. This second solution consists in making the walls rougher to increase friction. In our tests, we adopted this second method by coating the surfaces of the cone and the plane with a thin layer of aerosol glue, then a thin layer of bentonite powder. Other authors proceed by covering the surface of the plane and the cone with a rough sandpaper [6].

I.7.4 Rotating tool inertia

It has been shown that the use of an imposed stress rheometer could lead to measurement errors. These errors are due to a delay in the response of the tool to the stresses during the ascent or descent under stress. Krieger (1990) and subsequently Baravian and Quemada (1998), studied this type of error and they proposed a calculation method to eliminate them.

The principle of the correction by calculation is to break down the applied moment M into: I) a torque M_v necessary to overcome the forces of viscous origin generated by the sample

and II) a torque M_i necessary to overcome the inertia of the moving element of the rheometer in order to vary the speedΩ:

$M=M_v+M_i$

With

$$M_v = \eta_c.\frac{\Omega}{K}\Omega ET\, M_i = \frac{I.d\Omega}{dt} = 1\dot{\Omega} \qquad I\text{-}12$$

Where η_c the corrected local viscosity; I: the moment of inertia of the mobile tool;Ωrotor angular velocity;$\dot{\Omega}$:the angular acceleration of the rotor; Ψ:the angle of inclination of the cone in radians; $K = \frac{3.\Psi}{2\Pi.R^3}$:the constant relating to the cone-plane geometry and

$$\dot{\Omega} = \Psi.\frac{d\dot{\gamma}}{dt} = \Psi.\frac{\Delta\dot{\gamma}}{\Delta t} \qquad I\text{-}13$$

The actual corrected stress suffered by the sample is written as follows:

$$\tau_c = \eta_c.\dot{\gamma} \qquad I\text{-}14$$

In other words, during rapid variations in stress, and therefore in shear, the torque linked to the inertia of the moving part leads to certain measurement errors. Therefore, the actual viscous stress must be the subtraction of the stress displayed by the device and the term related to the inertia .In practice, we take this correction into account in a systematic way for old rheometers (Carri-Med).For the new generation (AR2000), you just have to pay attention to the driver software level by activating the "inertia correction" option.

Besides the calculation method, there is a second method in the literature to eliminate this type of error. The method consists in choosing the right measurement protocol by avoiding large accelerations and decelerations. We opted, on our side, for this second solution by using ramps of ascent and descent in long duration constraint [6].

I.8 Rotational rheometry

In the basic rotational test, the sample is subjected to constant or variable loading in one direction. The shear viscosity η is calculated from the measured data. The corresponding mechanical input and response parameters are listed in Tables I-2 and I-3 the basic parameters of the test can be represented schematically in terms of the two-plate model. An infinitesimal element of the measuring geometry is considered in this subclause (see FigureI-5). The two-plate model consists of two parallel plates, each with a surface area A and with a gap width h, between which the sample is located. The velocity of the lower plate is zero (v = 0). The upper plate is moved by a defined shear force F, which results in a velocity v. it is assumed that the sample between the plates consists of layers that move at different velocities of between v=0 and v [8].

Test type	Input	Response
Controlled rate (CR)	$\dot{\gamma}$	τ
Controlled stress (CS)	τ	$\gamma, \dot{\gamma}$
Controlled deformation (CD)	γ	τ

Table I-4: Rotational measurement — Rheological input and response parameters

Test type	Input		Response	
	Amplitude	Angular frequency or frequency	Amplitude	Phase angle
Controlled rate (CR)	$\dot{\gamma}_0$	ω or f	τ_0	
Controlled stress (CS)	τ_0		$\dot{\gamma}_0, \gamma_0$	δ
Controlled deformation (CD)	γ_0		τ_0	

Table I-5: Oscillatory measurement — Rheological input and response parameters

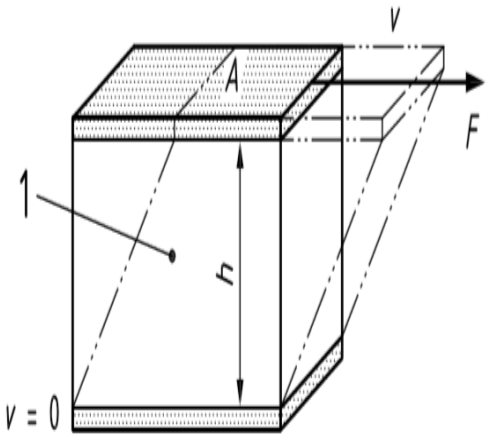

Figure I-6: Two plate model with a simplified schematic

1: sample

V: velocity

A: shear plane

h: gap width

F: shear force

With this model, the following parameters are calculated using Formulae (1) to (3):

$$\tau = \frac{F}{A} \qquad \text{I-15}$$

Where:

τ: is the shear stress, in Pascal

F: is the shear force, in newton

A: is the shear plane, in square

$$\dot{\gamma} = \frac{v}{h} \quad \text{I-16}$$

Where

$\dot{\gamma}$: is the shear rate, in reciprocal seconds

V: is the velocity, in meters per seconds

h: is the gap width, in meters

Based on the Newtonian law of viscosity, the shear viscosity can be calculated using Formula (3):

$$\eta = \frac{\tau}{\dot{\gamma}} \quad \text{I-17}$$

Where η is the shear viscosity, in Pascal multiplied by seconds [6].

I.9 Shear Rheometry: Drag Flows

I.9.1 Sliding Plates

Perhaps the simplest way of generating steady simple shear is to place one material between a large fixed plate and another plate moving at constant velocity, if inertial and edge effects can be neglected, then the flow is homogeneous and the equations of motion are identically satisfied. The shear strain, shear rate, and shear stress, respectively, will be simply [9].

$$B_{xy} = B_{12} = \gamma = \frac{\Delta x}{h} = \frac{v_0 t}{h} \quad \textit{I-18}$$

$$2D_{xy} = 2D_{12} = \dot{\gamma} = \frac{v_0}{h} \quad \text{I-19}$$

$$T_{xy} = T_{12} = \frac{f_x}{LW} \quad \text{I-20}$$

At very short times or at high frequency oscillation inertial effects cannot be neglected; especially when testing low viscosity samples. It takes a finite time for the velocity profile to develop. Schrage (1977) gives a simple criterion for the time to establish homogenous, simple shear flow

$$t_c \sim \frac{1}{w_c} = \frac{10\rho h^2}{\eta} \quad \text{I-21}$$

In principle, from the total thrust fy or from pressure measurements with sliding plates one could also determine T_{22}, but this does not appear to have been reported in the literature.

A major practical problem with this geometry is edge effects. With solids, unless L and w are much greater than h, buckling will occur it is very difficult to keep the two plates parallel for large strains and also for large normal forces. With liquids, the sample must be viscous enough not to run out, although if it is very viscous, it may also show the buckling and tearing problems typical for solids. The other obvious problem associated with liquids is achieving steady shear. As strain increases, the edge effects become more severe. Thus, most shear measurements on liquids are done with rotating geometries that have closed stream lines.

However, a number of studies have used shear plates. Van Wazer et al. (1963, p. 302) describes a device for studying asphalts that uses the sliding plate Most shear plate rheometers, however, use a double sample. This helps to prevent cocking and eliminates any normal stress effects. A shear sandwich geometry for solids that can be used in a standard tensile machine is shown in Figure I-**7**. The sample can be machined from a large block with a thin test section on each side and a thick section of sample used for applying the force (Sternstein et al., 1968). Rubber samples can be bonded to a metal block with adhesives (e.g., Goldstein, 1974).

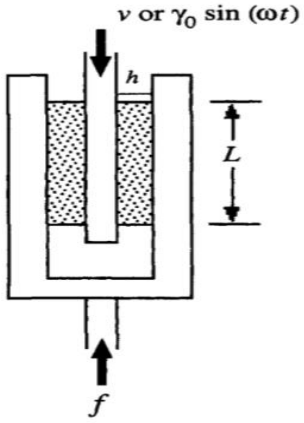

Figure I-8: Shear sandwich fixture for polymer melts, adhesives, or rubber.

A similar concept, shown in FigureI-9 , has been used for some time as a high shear rheometer for printing inks. As indicated in Figure I-10, a thin, wide film is pulled through a narrow gap filled with fluid. It is assumed that the flow will keep the film centered. The velocity is determined by timing marks on the film [9].

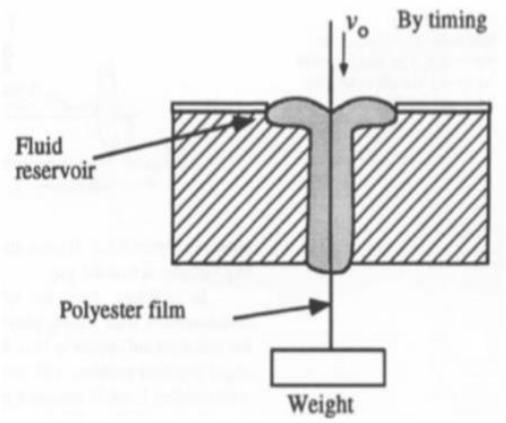

Figure I-11: Band viscometer used for high shear rate testing of inks and coatings.

I.9.2 The narrow-gap concentric-cylinder viscometer

If the gap between two concentric cylinders is small enough and the cylinders are in relative rotation, the test liquid enclosed in the gap experiences an almost constant shear rate. Specifically, if the radii of the outer and inner cylinders arer_0 and r respectively, and the angular velocity of the inner isΩ_1 (the other being stationary) the shear rate$\dot{\gamma}$ is given by

$$\dot{\gamma} = \frac{r_0 \Omega_1}{r_0 - r_1} \qquad \textit{I-22}$$

For the gap to be classed as "narrow" and the above approximation to be valid to within a few percent, the ratio of to must be greater than 0.97. If the couple on the cylinders is C, the shear stress in the liquid is given by

$$\sigma = \frac{c}{2\pi {r_0}^2 L} \qquad \text{I-23}$$

And from (14) and (15) we see that the viscosity is given by

$$\eta = \frac{c(r_0 - r_1)}{2\pi {r_0}^3 \Omega_1 L} \qquad \text{I-24}$$

Where L is the effective immersed length of the liquid being sheared. This would be the real immersed length, *l*, if there were no end effects. However, end effects are likely to occur if due consideration is not given to the different shearing conditions which may exist in any liquid covering the ends of the cylinders.

One way to proceed is to carry out experiments at various immersed lengths, I, keeping the rotational rate constant. The extrapolation of a plot of against I then gives the correction which must be added to the real immersed length to provide the value of the effective immersed length L. In practice, most commercial viscometer manufacturers arrange the dimensions of the cylinders such that the ratio of the depth of liquid to the gap between the cylinders is in excess of 100. Under these circumstances the end correction is negligible. The interaction of one end of the cylinder with the bottom of the containing outer cylinder is often minimized by having a recess in the bottom of the inner cylinder so that air is entrapped when the viscometer is filled, prior to making measurements. Alternatively, the shape of the end of the cylinder can be chosen as a cone. In operation, the tip of the cone just touches the bottom of the outer cylinder container. The cone angle (equal to tan-'[$^{(r_0 - r_1)}/_{r_0}$] - is such that the shear rate in the liquid trapped between the cone and the bottom is the same as that in the liquid between the cylinders. This arrangement is called the Mooney system, after its inventor [10].

I.9.3 The wide-gap concentric-cylinder viscometer

The limitations of very narrow gaps in the concentric-cylinder viscometer are associated with the problems of achieving parallel alignment and the difficulty of coping with suspensions containing large particles. For these reasons, in many commercial viscometers the ratio of the cylinder radii is less than that stated in (I.6.2), thus some manipulation of the data is necessary to produce the correct viscosity. This is a nontrivial operation and has been studied in detail by Krieger and Maroon (1954). Progress can be readily made if it is assumed that the shear rate relationship over the interval of shear stress/ shear rate in the gap can be described by the power-law model of eqn (I-25) [10].

$$\eta = k_2 \dot{\gamma}^{n-1} \qquad \text{I-26}$$

This is the well-known ‘power-law' model and n is called the power-law index.k_2 Is called the 'consistency' (with the strange units of Pa.s^n).

The shear rate in the liquid at the inner cylinder is then given by

$$\dot{\gamma} = \frac{2\Omega_1}{n(1 - b^{2/n})} \qquad \textit{I-27}$$

Where b is the ratio of the inner to outer radius($b = r_1/r_0$).Note that the shear rate is now dependent on the properties of the test liquid, unlike the narrow-gap instrument.

The shear stress in the liquid at the inner cylinder is given by

$$\sigma = \frac{2\Omega_1}{2\pi r_1^{\,2} L} \qquad \textit{I-28}$$

The value of can be determined by plotting C versus on a double-logarithmic basis and taking the slope at the value of under consideration

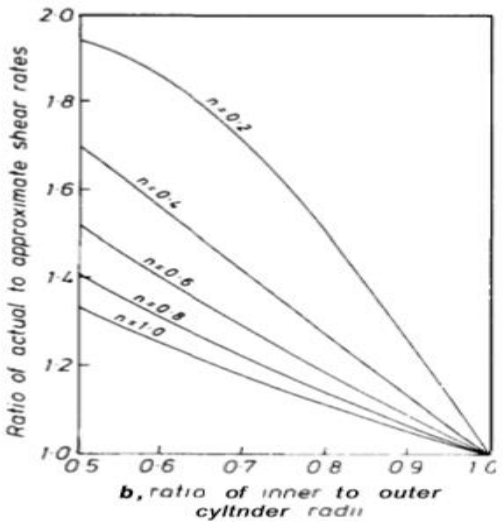

Figure I-12: Ratio of actual (eqnI-29) to approximate (eqn. I-30) shear rates at the rotating cylinder as a function of the ratio of the inner to the outer cylinder radii, with the power law index, as parameter.

The viscosity (measured at the inner-cylinder shear rate) is given by

$$\eta = \frac{c_n(1 - b^{2/n})}{4\pi r_1^{\,2} L \Omega_1} \qquad \textit{I-31}$$

The error involved in employing the narrow-gap approximation instead of the wide-gap expression, eqn (I-32). Is shown in Fig. (I-5). Clearly, using values of $b < 0.97$ gives unacceptable error when the liquid is shear-thinning ($n < 1$).

The lower limit of shear rate achievable in a rotational viscometer is obviously governed by the drive system. The upper limit, however, is usually controlled by the test liquid. One limit is the occurrence of viscous heating of such a degree that reliable correction cannot be made. However, there are other possible limitations. Depending on which of the cylinders is rotating, at a critical speed the simple circumferential streamline flow breaks down, either with the appearance of steady (Taylor) vortices or turbulence. Since both of these flows require more

energy than streamline flow, the viscosity of the liquid apparently increases. In practical terms, for most commercial viscometers, it is advisable to consider the possibility of such disturbances occurring if the viscosity to be measured is less than about 10 mpa.s [10].

I.9.4 Parallel Disks

The parallel disk geometry was suggested by Mooney (1934). The Mooney tester, which consists of a disk rotating inside a cylindrical cavity, is used extensively in the rubber industry (ASTM 01646). Russell (1946) first measured normal forces from the total thrust between two disks. Greensmith and Rivlin (1953) measured the pressure distribution, and Kotaka et al. (1959) used total thrust to study normal stresses in polymer melts. In many ways the flow is similar to the cone and plate. Most instruments are designed to permit the use of either geometry. However, in contrast to the cone and plate, flow between parallel disks is not homogeneous [9].

If we assume:

1. Steady, laminar, isothermal flow
2. $v_\theta(r,z)$only, $v_r = v_z = 0$
3. Negligible body forces
4. Cylindrical edge

Then the equations of motion reduce to

$$\theta: \frac{\partial \tau_{\theta z}}{\partial z} = 0 \qquad \textit{I-33}$$

$$z: \frac{\partial \tau_{zz}}{\partial z} = 0 \qquad \textit{I-34}$$

$$r: \frac{1}{r}\frac{\partial}{\partial r}(r\tau_{rr}) - \frac{\tau_{\theta\theta}}{r} = -\rho\frac{{v_\theta}^2}{r} \qquad \textit{I-35}$$

With one disk stationary and the other rotating at Q, assuming no slip at these surfaces and neglecting inertial forces, the velocity must be

$$v_\theta(r,z) = \frac{r\Omega_z}{h} \qquad \textit{I-36}$$

And thus

$$\dot{\gamma} = \frac{r\Omega}{h} \qquad \textit{I-37}$$

Shear strain:

$\gamma = \frac{\theta r}{h}$ *(nonhomogeneous, depends on position)* *I-38*

Shear rate at r = R

$$\dot{\gamma}_r = \frac{R\Omega}{h} \quad \textit{I-39}$$

Shear stress:

$$\tau_{12} = \tau_{\theta z} = \frac{M}{2\pi R^3}\left[3 + \frac{d \ln M}{d \ln \dot{\gamma}_R}\right] \quad \textit{I-40}$$

$\tau_a = \frac{2M}{\pi R^3}$ *Apparent or Newtonian shear stress* *I-41*

Representative shear stress:

$$\eta(\tau) = \eta_a(\tau_a) \pm 2\% \quad \textit{I-42}$$

For $\tau = 0.76\tau_a$ and $\frac{d\ ln\ M}{d\ ln\ \dot{\gamma}_R} < 1.4$

Normal stress

$$N_1 - N_2 = \frac{F_z}{\pi R^2}\left[2 + \frac{d \ln F_z}{d \ln \dot{\gamma}_R}\right] \quad \textit{I-43}$$

$$(F_z)_{inert} = 0.075\pi\rho\Omega^2 R^4 \quad \textit{I-44}$$

Chapter II: General description of the HR20

II.1 Introduction

Rheometry measurements are performed using a rheometer Depending on the type of rheometry, different designs of rheometers can be used, from acoustic extensional rheometers to cone and plate shear rheometers [11].

The rheometer applies a force to the sample and the resulting stress or strain is measured using a sensor device, such as a transducer or a displacement sensor. Some rheometers can be interfaced with computers for automated calculation of stress and strain factors from the measured forces to simply rheometry analysis [11].

II.2 Discovery Hybrid Rheometer (DHR)

The Discovery Hybrid Rheometer is designed to be an incredibly versatile platform for rheometry. It boasts TA Instruments' patented advanced drag cup motor, magnetic bearings, a force rebalance transducer and a True Position Sensor, all in a single-head hybrid device. This means it can perform direct stress and strain control measurements as well as regular force measurements. With a wide range of accessories, the Discovery Hybrid Rheometer also comes with the Smart Swap™ system for automatic detection and identification of devices to streamline your measurements [11].

II.3 Discovery Hybrid Rheometer Specification

II.3.1 DHR 20 Features

Features	HR20
Optical Encoder Dual Reader	●
DMA Mode	○
True Position Sensor (TPS)	●
Controlled stress (steady, transient, oscillation)	●
Controlled strain (steady, transient, iterative oscillation)	●
Direct Strain (oscillation)	●
Fast data collection	●
Normal Force measurements with FRT	●
Axial and tack testing	●
One-Touch-Away™ Display	●
ntegrated Sample Lighting	●
Fast Track	●
Autopilot	○

Table II-1: DHR 20 features

●Included ○Optional — Not Available [12]

II.3.2 Technical Specifications

Specification	HR20
Bearing Type, Thrust	Magnetic
Bearing Type, Radial	Porous Carbon
Motor Design	Drag Cup
Minimum Torque (nN.m) Oscillation	2
Minimum Torque (nN.m) Steady Shear	10
Maximum Torque (mN.m)	200
Torque resolution	0.1
Minimum Frequency (Hz)	1.0E-07
Maximum Frequency (Hz)	100
Minimum Angular Velocity (rad/s	0
Maximum Angular Velocity (rad/s)	300
Displacement Transducer	Optical encode
Optical Encoder Dual Reader	N/A
Displacement Resolution (nrad)	10
Step Time, Strain (ms)	15
Step Time, Rate (ms)	5
Normal/Axial Force Transducer	FRT
Maximum Normal Force (N)	50
Normal Force Sensitivity (N)	0.005
Normal Force Resolution (mN)	0.5

Table II-2: DHR Technical Specifications

[13]

II.3.3 Dynamic Mechanical Analysis (DMA) Mode

Specifications	
Motor Control	Force Rebalance Transducer
Minimum Force in Oscillation	3 mN
Maximum Axial Force	50 N
Minimum Displacement in Oscillation	0.01 μm
Maximum Displacement in Oscillation	100 μm
Axial Frequency Range	6×10^{-5}rad/s to 100 rad/s (10^{-5}Hz to 16 Hz)

Table II-3: DMA Mode specification

[13]

II.4 Discovery Hybrid Rheometer 20(HR20)

The HR 20 is an exceptional multi-purpose rheometer that can handle everything from cutting-edge research and development laboratories to continuous deployment in production control environments. With optional linear Dynamic Mechanical Analysis and the widest range of easy-to-use accessories, the HR 20 is ready to handle any set of challenges, from complementing shear rheology to testing solids under tension, compression or bending [14].

Figure II-1: discovery hybrid rheometer 20

II.5 Description

Advances in core measurement technology enable more sensitive measurements with superior precision. This empowers you to measure lower viscosities and weaker liquid and soft-solid structure, while consuming less material. Superior dynamic performance gives a higher level of accuracy in measurements of G' and G" so you can make decisions quickly, with confidence [14].

Thoughtful hardware and software design results in a complete system that simplifies every user interaction. Routine functions are faster and more intuitive, so you can accomplish more with less training [14].

The performance of the Discovery Hybrid Rheometer is supported by the widest range of powerful, easy-to-use environmental systems and accessories that allow you to replicate demanding environmental conditions, incorporate complementary simultaneous measurements, or extend your rheometer beyond conventional shear rheology [14].

II.6 Measurement sensitivity and accuracy

II.6.1 Measure the lowest stresses and smallest sample volumes with revolutionary torque sensitivity

Unrivaled low torque sensitivity empowers you to measure lower viscosities and weaker intermolecular structures while using lower sample volumes

All Discovery Hybrid Rheometers feature TA's patented Magnetic Thrust Bearing, which reduces basic system friction by 70% compared to traditional designs. By eliminating the contributions of high-pressure turbulent air flow from the measurement system, lower torques can be measured reliably and accurately

The unparalleled sensitivity of the magnetic thrust bearing is coupled with the NEW improved Advanced Drag Cup Motor. Enhanced torque precision increases the accuracy of every measurement, especially at low torques [12].

II.6.2 Advanced Strain and Stress Control

The Discovery Hybrid Rheometer performs the experiment you want, whether stress-controlled, strain-controlled, or both. State-of-the-art high-speed electronics and the responsive Advanced Drag Cup Motor provide the fastest transient responses and accurate control in any type of deformation. Direct Strain oscillation provides real-time strain control at every point of the oscillatory measurement

Responsive strain control ensures rapid data collection so you can characterize materials that are undergoing thermal, chemical, or structural transitions. Highly accurate deformation control (stress or strain) also ensures the highest data quality, particularly when evaluating materials that show a non-linear response at very large amplitudes [12].

II.6.1 Dynamic Mechanical Analysis (DMA)

Backed by over four decades of TA Instruments' expertise in rotational rheology and linear DMA measurements, the Discovery Hybrid Rheometers DMA Mode adds a new dimension for testing solid and soft-solid materials. Now in addition to the most sensitive and accurate rotational shear measurements, the DHR can deliver accurate linear Dynamic Mechanical Analysis (DMA) data. Axial DMA complements solid torsion testing by providing a direct measure of the modulus of elasticity, or Young's Modulus (E). The new DMA mode is ideal for identifying a material's transition temperatures and provides reliable measurements over the instrument's full range of temperatures [15].

II.6.2 Control and analysis software

II.6.2.1 Trios software

II.6.2.1.1 Trios Features

- Control multiple instruments with a single PC and software package
- Overlay and compare results across techniques including DSC, TGA, DMA, SDT, TMA and rheometers
- One-click repeated analysis for increased productivity
- Automated custom report generation including: experimental details, data plots and tables, analysis results
- Convenient data export to plain-text, CSV, XML, Excel, Word, PowerPoint,

And image formats

- Optional TRIOS Guardian with electronic signatures for audit trail and data integrity including U.S. FDA 21 CFR 11 compliance [12].

II.6.2.1.2 What trios software provides

- Trios for the discovery hybrid rheometer features two powerful user interfaces that present users with what they need to collect the data they want.
- Trios express helps users to design the most common measurements quickly and easily. Simple forms and sensible defaults streamline the process of experiment design and execution.
- Trios unlimited gives you complete control. A robust set of detailed experimental controls and data collection options ensures that you will be able to design the experiment you envision and collect the data you need [12].

II.6.2.2 Complete Data Record

The advanced data collection system automatically saves all relevant signals, active calibrations, and system settings. Waveforms for each data point may be displayed as Lissajous plots and provide a visual representation of the stress-strain relationship. This comprehensive set of information is invaluable for method development, procedure deployment, and data validation [12].

II.6.2.3 Complete Data Analysis Capabilities

A comprehensive set of relevant tools are available for real-time data analysis, even during experiments. Gain actionable insights into your material behaviour through a powerful and versatile set of features seamlessly integrated into trios [12].

II.6.2.3.1 All Standard Analyses

- Onset and end set analysis
- Signal maximum and minimum
- Signal change
- Modulus crossover
- Curve values at specific X or Y points

- 1st and 2nd derivatives
- Area under the curve
- Peak height
- Peak integration and running integral
- Mathematical fitting: straight line, polynomial, or exponential
- Statistical functions [12].

II.6.2.3.2 Advanced Analysis Capabilities

- More than 10 flow models including automatic model selection based on best fit to experimental data
- Time-Temperature Superposition (TTS) analysis with automatic curve shifting and Master curve generation
- Activation Energy calculation
- WLF coefficient calculation
- Convert between temperature ramps and frequency sweeps
- Cole-Cole, Van Gurp-Palmen, and Lissajous plots
- Built-in models for: discrete and continuous relaxation or retardation spectra, Oldroyd and Spriggs models
- Creep ringing analysis by Kelvin, Maxwell, or Jeffreys models
- Viscoelastic transformations to interconvert between oscillation, stress relaxation, stress growth, creep, relaxation spectra, retardation spectra, and memory functions.
- Advanced custom analysis with user-defined variables and models
- Cox-Merz: $\eta^*(\omega) \rightarrow \eta(\ )$
- Fluid Inertia Correction
- Rabinowicz Correction
- Direct Creep – Oscillation conversion
- Discrete Fourier Transformation (DFT)
- Window Correlation [12].

II.7 DHR temperature systems and accessories

II.7.1 Peltier plate

Advanced, Standard and Stepped Peltier Plates offer a temperature range of -40 °C* to 200 °C, heating rates up to 50 °C/min, and temperature accuracy of 0.1 °C. Four Peltier heating elements are placed directly in contact with a thin, 80 mm diameter, copper disc with an extremely rugged, hardened surface. A platinum resistance thermometer (PRT) is placed at the exact center, ensuring accurate temperature measurement and control. The unique design provides for rapid, precise, and uniform temperature control over the entire 80 mm diameter surface. This allows for accurate testing with standard geometries up to 60 mm in diameter [15].

- Features and Benefits:
  - Smart Swap™ technology
  - Wide Temperature Range: -45 °C to 200 °C
  - Widest Continuous Temperature Range
  - Accurate Temperature Control: ±0.1 °C
  - Hardened Chrome Surface
  - Standard, Stepped, and Dual Stage Models
  - Plates and Cones up to 60 mm in Diameter
  - Disposable Plates
  - Large Variety of Geometry Materials and Types
  - Fully Accessorized
- Smart Swap technology:

Peltier plates can be used with an extensive range of TA Instruments unique Smart Swap geometries (1) with automatic recognition. Cones and plates come standard in a variety of sizes, cone angles and material types. Custom geometries of non-standard sizes, materials, and surface finishes (such as sandblasted or Teflon®-coated) are available upon request [15].

- Upper Heated Plate (UHP):

The UHP is a temperature option designed for use with Peltier plates to eliminate vertical temperature gradients in samples. These thermal gradients can become significant above 50 °C

and lead to errors in absolute rheological data. The UHP is the most advanced non-contact heating system available, using patented heat spreader technology (1) to deliver maximum heat transfer efficiency and patented active temperature control (2) for direct measurement and control of the upper plate temperature. The UHP has a maximum operating temperature of 150 °C and the lower temperature can be extended using liquid or gas cooling options.(Note: to extend the upper heated temperature to 200 °C, see Electrically Heated Plates option) [15].

II.7.2 Peltier Concentric Cylinder

The Peltier Concentric Cylinder Temperature System combines the convenience of Smart Swap™ and Peltier heating technology with a wide variety of cup and rotor geometries. Concentric Cylinder geometries are commonly used for testing low viscosity fluids, dispersions or any liquids that are pourable into a cup. Examples of materials suitable for Concentric Cylinder include low concentration polymer solutions, solvents, oils, drilling mud, paint, varnish, inkjet ink, ceramic slurries, pharmaceutical suspensions and cough medicine and baby formula, foams, and food and dairy products such as milk, sour cream, juices, salad dressings, and pasta sauce [15].

II.7.3 Pressure Cell

The Pressure Cell is a sealed vessel that can be pressurized up to 138 bar (2,000 psi), over a temperature range of -10 °C to 300 °C. It can be used either in self-pressurizing mode, in which the pressure is produced by the volatility of the sample, or by externally applying the pressurization, typically with a high pressure tank of air or nitrogen gas. The accessory includes a 26 mm conical rotor; optional vane and starch rotors are also available. All necessary plumbing and gauges are included as a manifold assembly. The Pressure Cell is ideal for studying the effect of pressure on rheological properties, as well as studying the materials that volatilize under atmospheric pressure [15].

II.7.4 Electrically Heated Concentric Cylinder (EHC)

The Electrically Heated Concentric Cylinder system enables concentric cylinder rheological measurements over the broad range of temperatures from ambient to 300 °C. Perfect for high-temperature testing of low viscosity liquids, the Electrically Heated Cylinder also supports high-temperature and pressure studies in conjunction with the popular Pressure Cell.

These combined high-pressure and temperature investigations are ideal for characterizing fluids under down-hole conditions relevant to mining and oil recovery operations [15].

II.7.5 Electrically Heated Plate (EHP)

The EHP provides active heating and cooling of parallel plate and cone and plate geometries. With standard and disposable systems, it is ideal for rheological characterization of polymer melts and thermosetting materials up to a maximum temperature of 400 °C. The optional Gas Cooling Accessory extends the minimum temperature to -70 °C. Standard features include 25 mm diameter parallel plate geometry, environmental cover, and heated purge gas. An optional clear cover is available for sample viewing and for use with the Camera Viewer option. The EHP offers Active Temperature Control (ATC) making it the only electrically heated plate system capable of direct temperature control of the upper and lower plates (See ATC Section on page 16 for more details on this advanced technology). The upper EHP can be used with lower Peltier Plates for temperature control to 200 °C and as temperature control to 150 °C for UV curing options [15].

II.7.6 Environmental Test Chamber (ETC)

The ETC is a high temperature Smart Swap™ accessory that employs a combination of radiant and convective heating and has a temperature range of -160 °C to 600 °C with heating rates up to 60 °C/min. This hybrid temperature control design provides fast response and temperature stability over a continuous range of 760 °C. The ETC is a very popular option for polymer applications and can be used with parallel plate, cone and plate, disposable plate, rectangular torsion and DMA clamps for solids, and the SER3 for extensional viscosity measurements. Typical materials that can be tested include thermoplastics, thermosets, elastomers, caulks and adhesives, solid polymers, asphalt binder, and oils and greases [16].

II.7.7 Orthogonal Superposition

Orthogonal Superposition (OSP) provides direct measurements of viscoelasticity under simultaneous shear, for complete characterization of materials throughout all stages of use. This new dimension in rheological testing bridges the gap between oscillation and flow, measuring a material’s viscoelastic behaviour under the same shear conditions experienced during critical processes such as mixing, extrusion, dispensing, pouring, pumping or spreading [17].

II.7.8 Relative Humidity Accessory

The DHR-RH Accessory is a new environmental system for the Discovery Hybrid Rheometer that enables accurate control of sample temperature and relative humidity. The DHR-RH Accessory employs a custom-designed humidity and temperature chamber that is optimized for rheological measurements. The accessory provides stable, reliable control of temperature and humidity over a wide range of operating conditions and successfully prevents condensation, a common occurrence in controlled-humidity environments which makes accurate control of relative humidity impossible [18].

II.7.9 Modular Microscope Accessory (MMA)

The Modular Microscope Accessory (MMA) enables complete flow visualization – including counter-rotation – with simultaneous rheological measurements on a Discovery Hybrid Rheometer. A high-resolution camera collects images at up to 90 fps coupled with industry-standard microscope objectives that provide magnification up to 100×. Illumination from a blue-light LED can be coupled with a cross-polarizer or dichroic splitter for selective illumination or fluorescence microscopy [19].

II.7.10 Small Angle Light Scattering

The Small Angle Light Scattering (SALS) System is an option for simultaneously obtaining rheological and structural information, such as particle size, shape, orientation and spatial distribution. It is available for the DHR-3 and DHR-2 Rheometers. The option incorporates TA Instruments' Smart Swap™ technology, bringing a new level of speed and simplicity for making simultaneous rheology and SALS measurements. The system can be installed, aligned, and ready for measurements in as little as five minutes. It features patented Peltier Plate temperature control (1) and the scattering angle (θ) range over which measurements can be made is ~ 6° to 26.8°. The scattering vector range (q) is 1.38 μm-1 to 6.11 μm-1 and the length scale range is about 1.0 μm to ~ 4.6 μm [20].

II.7.11 Electro-Rheology

Lector-Rheological, or "ER", fluids are suspensions of extremely fine non-conducting particles in an electrically insulating fluid. These materials show dramatic and reversible rheological changes when the electric field is applied. The Discovery Hybrid Rheometer ER accessory provides the ability to characterize ER fluids up to 4,000 volts using either parallel

plate or concentric cylinder geometries. The accessory is available for all DHR models and compatible temperature systems include the popular Peltier Plate (-40 °C to 200 °C) and Peltier Concentric Cylinder (-20 °C to 150 °C). A custom waveform and function generator enables the user to program a wide range of voltage profiles directly in TRIOS Software. Voltage Profiles include: constant voltage, step voltage, ramp voltage, sine wave voltage function, triangle wave voltage function, and wave functions with DC offsets. There are no limitations to the type of rheological experiments that can be performed with this accessory. A protective polycarbonate shield with trigger interlocks is also included with the accessory to provide safety from electrical shocks [21].

II.7.12 Starch Pasting Cell (SPC)

The Starch Pasting Cell (SPC) provides a more accurate and powerful tool to characterize the gelatinization of raw and modified starch products, as well as the properties of the starch gels. It can also be used for characterizing many other highly unstable materials. It uses an innovative impeller design for mixing, reduction of water loss, and control of sedimentation during testing. The actual sample temperature is measured and controlled in a temperature chamber with heating/cooling rates up to 30 °C/min [22].

II.7.13 Interfacial Rheology

Rheometers are typically used for measuring bulk or three-dimensional properties of materials. In many materials, such as pharmaceuticals, foods, personal care products and coatings, there is a two-dimensional liquid/liquid or gas/liquid interface with distinct rheological properties.

Only TA Instruments offers a choice of different devices for the most flexibility and widest range of quantitative interfacial rheology measurements. The options include a patented Double Wall Ring (DWR) system for quantitative viscosity and viscoelastic information over the widest measurement ranges, a Double Wall Du Noüy Ring (DDR) for samples available in limited volumes, and a traditional Bicone for interfacial viscosity measurements.

The new Interfacial Exchange Cell accessory further expands the capabilities of the DWR geometry through a controlled exchange of the sub-phase composition during interfacial measurements [23].

II.7.14 Interfacial Exchange Cell

The Interfacial Exchange Cell expands TA Instruments' patented offerings for interfacial rheology by providing the ability to directly manipulate the composition of the lower liquid layer (sub phase) during rheological measurements. This unique capability enables the characterization of the interfacial response to a modified sub phase composition, opening possibilities for quantifying the effects of changes in pH, salt, or drug concentration, or the introduction of new proteins, surfactants, or other active ingredient [24].

II.7.15 Optics Plate Accessory (OPA)

The OPA is an open optical system that permits basic visualization of sample structure during rheological experiments, revealing important insights about material behaviour under flow. An open platform with a borosilicate glass plate provides a transparent optical path through which the sample can be viewed directly. This enhances the understanding of a range of materials, especially suspensions and emulsions. The accessory is easy to use and install, accommodates diverse optical systems, and offers accurate temperature control over a wide range for flow visualization and microscopy [25].

II.7.16 UV Curing Accessories

UV-curable materials are widely used for coatings, adhesives, and inks. When these materials are exposed to UV radiation, a fast cross-linking reaction occurs, typically within less than a second to a few minutes. Two Smart Swap™ accessories for rheological characterization of these materials are available for the DHR rheometer. One accessory uses a light guide and reflecting mirror assembly to transfer UV radiation from a high-pressure mercury light source. The second accessory uses self-contained light emitting diodes (LED) arrays to deliver light to the sample. The UV Curing accessories include 20 mm quartz plate, UV light shield, and nitrogen purge cover. Optional temperature control using the Upper Peltier Plate (UPP) to a maximum of 150 °C is available. Disposable plates are available for hard UV coatings, which cannot be removed from the plates once cured [26].

II.7.17 Dielectric Measurement

The Dielectric Accessory extends material characterization capabilities by providing an additional technique similar to dynamic mechanical. In dielectric analysis, an oscillation electrical field (AC Field) is used as opposed to mechanical force (stress) and the oscillating

strain is a stored charge (Q) in the sample. The technique measures the degree to which the sample is storing a charge (capacitance) or passing a charge (conductance) through its bulk. The DHR provides a flexible platform for easy test setup and calibration, and data accuracy through standard features such as the Environmental Test Chamber, axial force control, and gap temperature compensation routines. Dielectric analysis is a very powerful technique for characterizing polar materials such as PVC, PVDF, PMMA, and PVA, for phase separating systems, and for monitoring curing kinetics of materials such as epoxy and urethane systems. Dielectric analysis extends the measurable frequency range over traditional dynamic mechanical analysis which is typically limited to 100 Hz [2].

II.7.18 Immobilization Cell

The new Immobilization Cell Accessory for the Discovery Hybrid Rheometer permits the characterization of drying, retention, and immobilization kinetics of paints, coatings and slurries. Solvent is dewatered from the sample through a paper substrate affixed to a perforated lower plate under controlled temperature and vacuum. Rheological changes in the sample during this immobilization process are simultaneously quantified through an oscillatory time sweep test with controlled axial force. Solid state Peltier heating and cooling provides faster, more stable temperature control, and is easier to use than competitive designs that rely on liquid-based temperature control. The DHR Immobilization Cell is a Smart Swap™ system that is extremely easy to install, use, and clean [28].

II.7.19 Tribo-Rheometry

Tribology is defined as the study of interacting surfaces undergoing relative motion. The new Tribo-Rheometry Accessory, available for all DHR models, enables the capability to make coefficient of friction measurements between two solid surfaces under dry or lubricated conditions. The unique self-aligning design ensures uniform solid-solid contact and axial force distribution under all conditions. A modular set of standard and novel geometries offers a choice of different contact profiles and direct simulation of end-use conditions. Accurate and precise control of axial force, rotational speed, and temperature inherent to TA Instrument rheometers provides for the best and widest range of friction measurements.

The advanced TRIOS software offers easy setup and control of Tribo-rheometry tests and contains a complete set of variables required for data analysis including the coefficient of friction

(μ), load force (FL), friction force (FF) and Gumbel number (GU). These may be used to construct Stribeck curves, static friction measurements, or explore specific combinations of temperature, contact force, and motion [29].

Chapter III: Materials and methods

III.1 Introduction

Historically, jams originated as an early effort to preserve fruit for consumption during the off-season. It is an intermediate moisture food prepared by boiling fruit pulp with sugar, pectin, acid and other ingredients (preservatives, colouring and flavouring substances) until obtaining a reasonably thick consistency [30].

III.2 Jam production

III.2.1 Jam

A solid gel made from the pulp of a single fruit or mixed fruits. The fruit content must be at least 40%. In mixed fruit jams the first-named fruit must be at least 50% of the total fruit. The total sugar content must be no less than 68%. In tropical climates, 70% sugar is preferable [31].
There are two basic methods of making jams and jellies. The standard method, which does not require added pectin, works best with fruits naturally high in pectin. The other method, which requires the use of commercial liquid or powdered pectin, is much quicker. Because the gelling ability of various pectin differs [32].

III.2.2 Jam making

Jam making is quite a technical process. It requires a large amount of sugar (equal quantities of fruit and sugar), citric acid (or lemon juice) and pectin. It also requires considerable amounts of fuel to boil the mixture to the required consistency and final moisture content. These ingredients and the fuel can be quite expensive. In addition, glass jars are required for packaging, which may be difficult and expensive to acquire. (Jam is sometimes packaged in plastic containers, but this reduces its keeping quality considerably, and makes it prone to rapid spoilage) [33].

III.2.3 Pectin

Consists mainly of the partial methyl esters of polygalacturonic acid and their sodium, potassium, calcium and ammonium salts; obtained by extraction in an aqueous medium of appropriate edible plant material, usually citrus fruits or apples; no organic precipitants shall be used other than methanol, ethanol and isopropanol; in some types a portion of the methyl esters may have been converted to primary amides by treatment with ammonia under alkaline conditions. Sulfur dioxide may be added as a preservative. The commercial product is normally diluted with sugars for standardization purposes. In addition to sugars, pectins may be mixed with

suitable food-grade buffer salts required for pH control and desirable setting characteristics. The article of commerce may be further specified as to pH value, gel strength, viscosity, degree of esterification, and setting characteristics [34].

III.2.4 Apricot Jam production

III.2.4.1 Preparation of the fruit

Fruit should be washed in clean water, peeled and the stones removed. Fruit should be as fresh as possible and slightly under-ripe. [31].

III.2.4.2 Blanching

Blanching is a thermal treatment in hot water or steam aimed to inactivate oxidative enzymes naturally present in fruits and responsible for off-flavors, color change, and chemical reactions during the further processing steps and storage. This first thermal step is very important when the fruits are further processed. This thermal step also helps to destroy microorganisms (bacteria, yeasts, and molds), clean the fruits, brighten the color, and expel trapped air in the intercellular regions. The main enzymes affected by blanching are peroxidase, polyphenol oxidase, catalase, lipoxygenase, and chlorophylase.

Blanching is carried out by different means such as hot water, steam [43], high pressure, infrared-dry blanching , ohmic , fluidized bed with steam, whirling bed with a mix of hot air and steam, individual quick blanching system, combined with ozone. Hot-water blanching is by far the most popular and commercially adopted process for its simplicity and economic reasons. The microbial quality of the blanching water must also be observed because the high temperature could select thermophilic bacteria. The main problem of water blanching is the leaching of important nutrients such as vitamins and pigments.

Blanching efficiency greatly depends on the size and shapes of the fruits. The thermal product conductivity governs the heat transfer in the matrix, and in the case of unsteady state, the thermal diffusivity is introduced in the heat transfer equations. The thermal diffusivities of fruits vary between 1×10^{-7} and 1.8×10^{-7} m s $^{-2}$: the heat transfers are 1000 times faster than the mass transfer of micronutrients in fruits. It is also important to note that as the thermal transfer time depends on the fruit pieces, size reduction is interesting in terms of heat and mass transfers [35].

III.2.4.3 Sulphuring

Apricots are treated with sulphur dioxide to help them keep a bright orange colour. It is not essential to treat with sulphur, but if you have some, it will also help to preserve the fruit [33].

III.2.4.4 Drying

Preserving food requires the control of enzymes and microorganisms. Microorganisms which grow rapidly on raw or fresh food products can be controlled by drying because the lack of water limits the growth of microorganisms; however, drying does not kill the microorganisms. Inactivation of enzymes in the fruit or vegetable is usually controlled by a pretreatment. Enzymes can catalyze undesirable flavor and color changes [36].

III.2.4.4.1 Sun Drying

Sun drying is the evaporation of water from products by sun or solar heat, assisted by movement of surrounding air. To be successful, it demands a rainless season of bright sunshine and temperatures above 98° F coinciding with the period of product maturity. Sun drying requires considerable care. Products must be protected from insects and must be sheltered during the night. This method is relatively slow, because the sun does not cause rapid evaporation of moisture. Reduced drying times may be achieved by using a solar dryer. Plans are available from your county Extension office [36].

III.2.4.4.2 Air Drying

Air drying is an alternative to sun drying. Enclosing produce in a paper bag protects it from dust and other pollutants [36].

III.2.4.4.3 Dehydrators

Dehydrators with thermostatic controlled heat and forced air circulation are available from a number of commercial sources. They can also be constructed from a variety of materials available to the home carpenter. Dehydrators require: 1) an enclosed cabinet, 2) a controlled source of heat, and 3) forced air to carry away the moisture. Venting to allow intake and exhaust of air is necessary [36].

III.2.4.4.4 Oven Drying

Oven drying is harder to control than drying with a dehydrator; however, some products can be quite successfully dried in the oven. It typically takes two to three times longer. Thus, the oven is not as efficient and uses more energy [36].

III.2.4.5 Pulp/Juice Extraction

To produce a clear juice for jelly, the juice should be filtered using a muslin cloth bag. The pH of the juice or pulp should be 3.0 to 3.3. It is measured using a pH meter and adjusted by adding citric acid or sodium bicarbonate (if the acidity is too high, for example with limes). Pectin is added to the pulp at this stage [31].

The washed apricots were dried and then processed immediately for extraction of pulp. For pulp extraction electric blender of good quality was used, pulp was separated from the stones of fruit. The extracted pulp was then pasteurized. Pulp was placed in water bath at a temperature of 82oC for 30 minutes to reduce the microbial load. After pasteurization chemical preservatives was mixed with extracted pulp [37].

III.2.4.6 Added Ingredients

III.2.4.6.1 Pectin

Pectins are naturally present in fruits. Some fruits contain higher levels than others. The richest sources are citrus peels, passion fruit and apple. Strawberries and melon contain low levels. In general, the pectin level decreases as the fruit matures. Low-pectin fruits are often mixed with high pectin fruits to achieve the correct level. Pectin is needed to make the fruit set into a gel [31].

Although it is possible to get a good preserve using the pectin in the fruit, it is better to buy pectin powder or solution and add a known amount to the fruit juice or pulp. This will produce a standardised gel each time and there will be less risk of a batch failing to set [31].

Pectin can be bought, either as a light brown powder or a dark liquid concentrate. It is usually supplied as '150 grade' (or 150 SAG) which indicates the ratio of the weight of sugar to pectin that will give a standard strength of gel when the preserve is boiled to 65% soluble solids. 5 SAG is normally enough to produce a good gel [31].

There are two main types of pectin:

1. High methoxyl (HM)
2. Low methoxyl (LM).

High methoxyl pectins form gels in high solid jams (above 55% solids) and in a pH range 2.0-3.5.

Low methoxyl pectins do not need sugar or acid to form a gel, instead they use calcium salts. LM pectins form a gel with a wide range of solids (10-80%) within a broad pH range of 2.5- 6.5.

Pectins may be either slow or fast setting. For most preserves a slow setting type is needed so it can set in the jar. If pieces of fruit are suspended in the gel, or if large volumes of jam are being made, a fast setting pectin is needed. In both types, the concentration of pectin varies from 0.2-0.7% depending on the type of fruit being used [31].

III.2.4.7 Heat Treatment

Different ratios of sweeteners non caloric were taken and used for jam preparation according to the formula and procedure of Awan and Rehman (1999). The jam samples were cooked in the open steel container. The fruit pulp were taken in an open container and heated. At the same time commercial grade pectin with small amount of non-caloric sweeteners were dissolved separately and added to the mixture in container. Preservatives and color was added at the end of cooking [37].

III.2.4.8 Filling

The jars should be clean and sterilised. The ideal temperature for pouring is 82-85°C. Hotter than this and condensation will form under the lid. This will drop down and dilute the jam, allowing mould to grow. Colder than this and the jam will be difficult to pour. Containers should be filled to about 9/10 ths of their volume [31].

III.2.4.9 Apricot jam storage

All preserved fruits should be stored in a cool dry environment not susceptible to temperature change. When items go through temperature changes of cool to warm and vice versa, the moisture in the air tends to condensate inside the packages. This moisture allows mold to grow and your jam or jelly to spoil. Refrigeration is highly recommended, but only after the jam or jelly has been opened and the freshness seal has been broken [38].

III.3 Experimental protocols

III.3.1 Initial device preparation

1. Removal of impurities from the place designated for the sample:

Figure III-1: Removal of impurities

2. Check tool type and balance:

The program has a feature that allows checking the type and balance of the tool.

III.3.2 Protocol 1(shear rates control)

The protocol 1 is accomplished in five steps:

To control the memory effect of the sample, we subjected the sample to a pre-shear under imposed shear rate (10 1/s)) for 10 seconds.

Subsequently, the sample is left to rest, still under the measurement geometry, for 10 minute. This would allow the suspension to recover, at least partially, its initial structure.

After the rest time, a succession of shear rates is imposed on the sample according to a rising ramp of 240 seconds, a maximum shear rate level for 10 minutes and a falling ramp of 240 seconds.

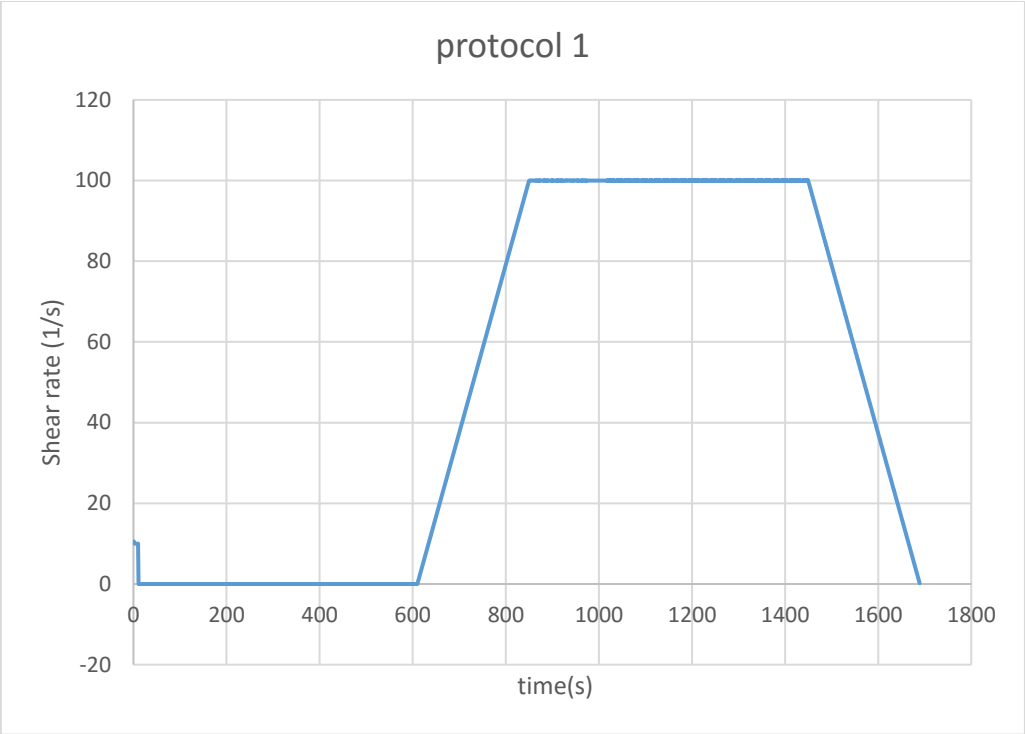

Figure III-2: Protocol 1(shear rates control)

III.3.2.1 Con plate geometry

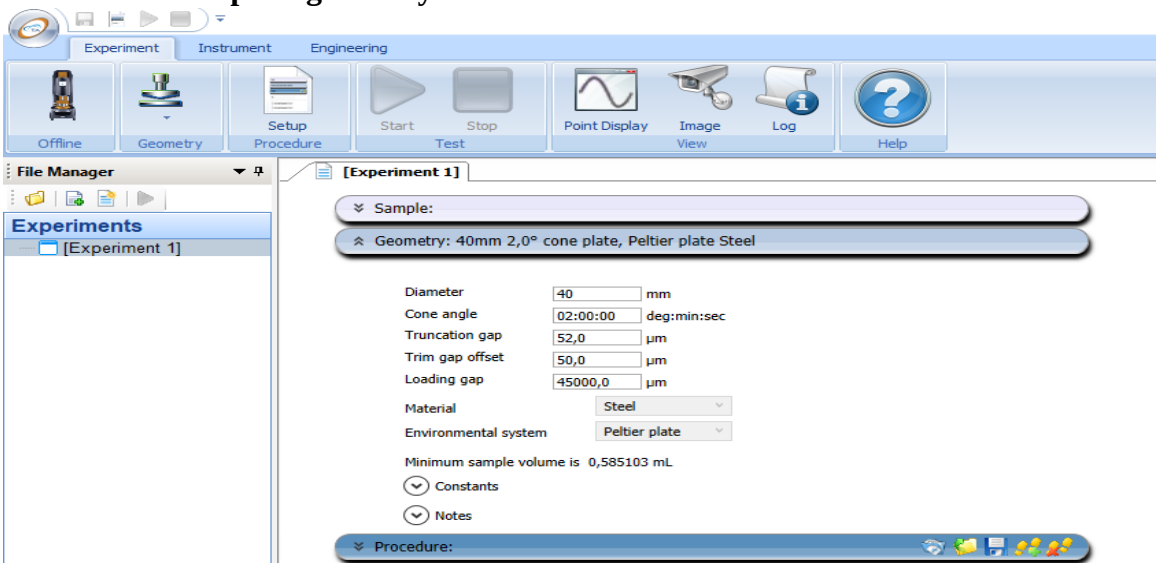

Figure III-3: Con plate geometry dimension

1. Peak hold 1: 20℃ ;10s ;10 1/s :

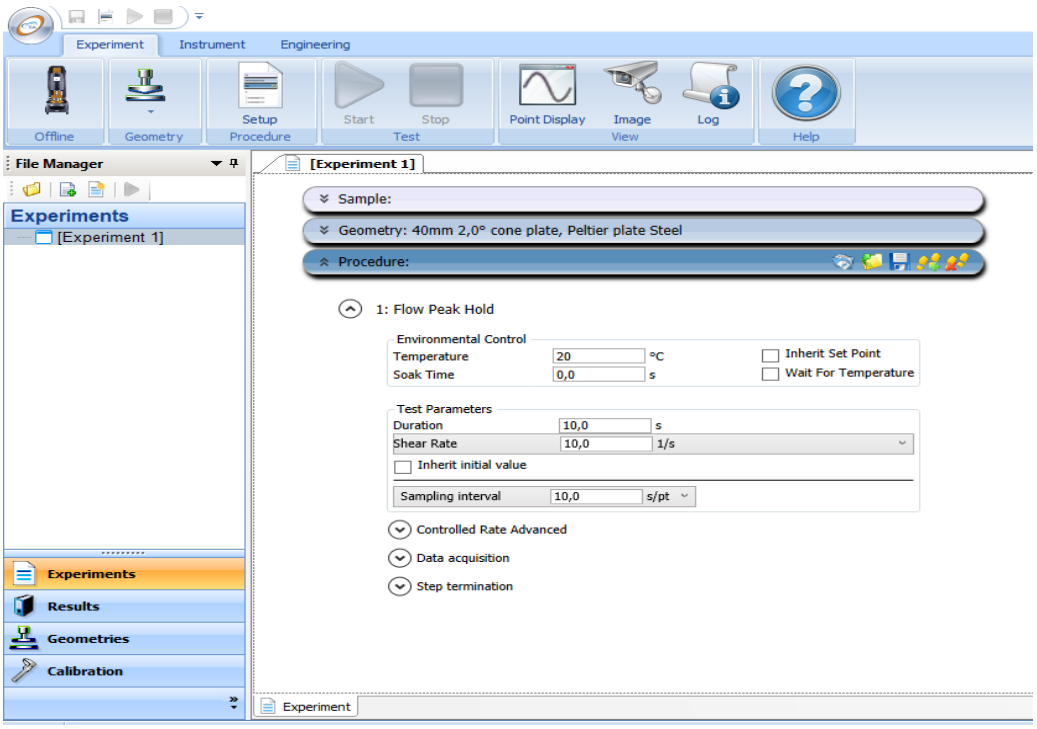

Figure III-4: Con plate geometry Peak hold 1

2. Peak hold 2: 20℃ ;600s ;0 1/s :

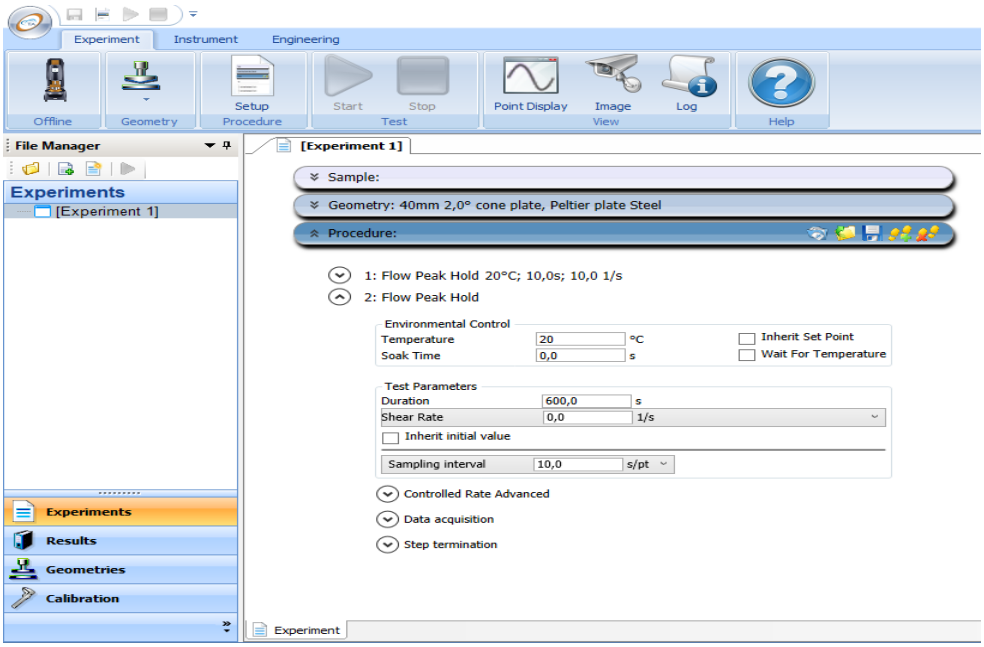

Figure III-5: Con plate geometry Peak hold 2

3. Flow ramp 1: 20℃ 240s;0 to final 100 1/s :

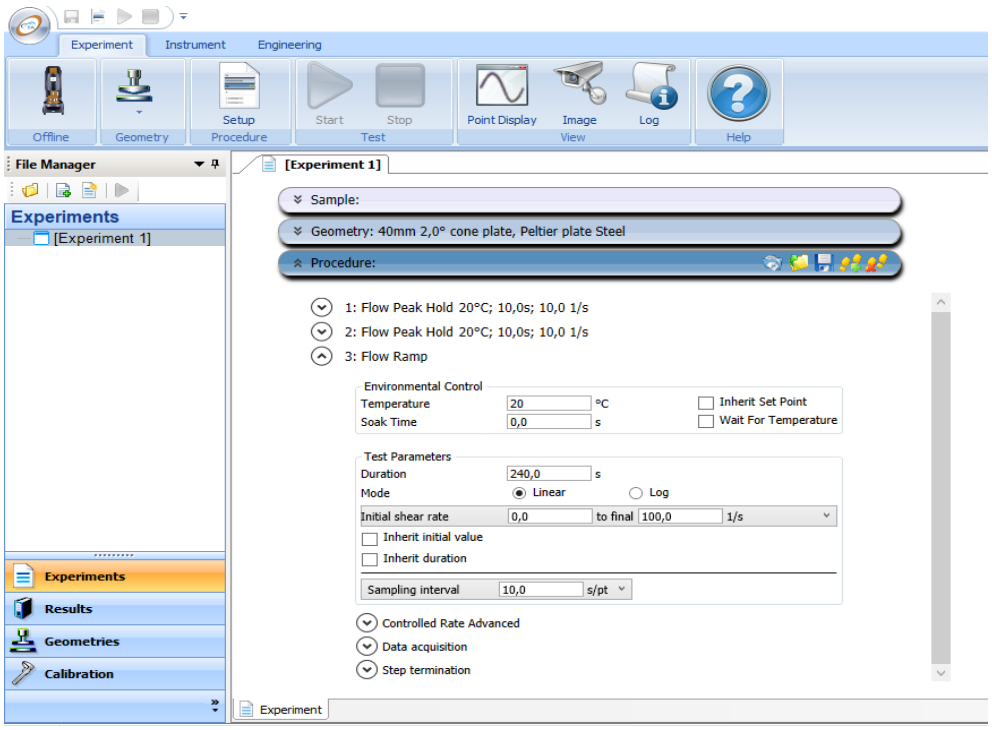

Figure III-6: Con plate geometry Flow ramp 1

4. Peak hold 3: 20℃ ;600s ;100 1/s :

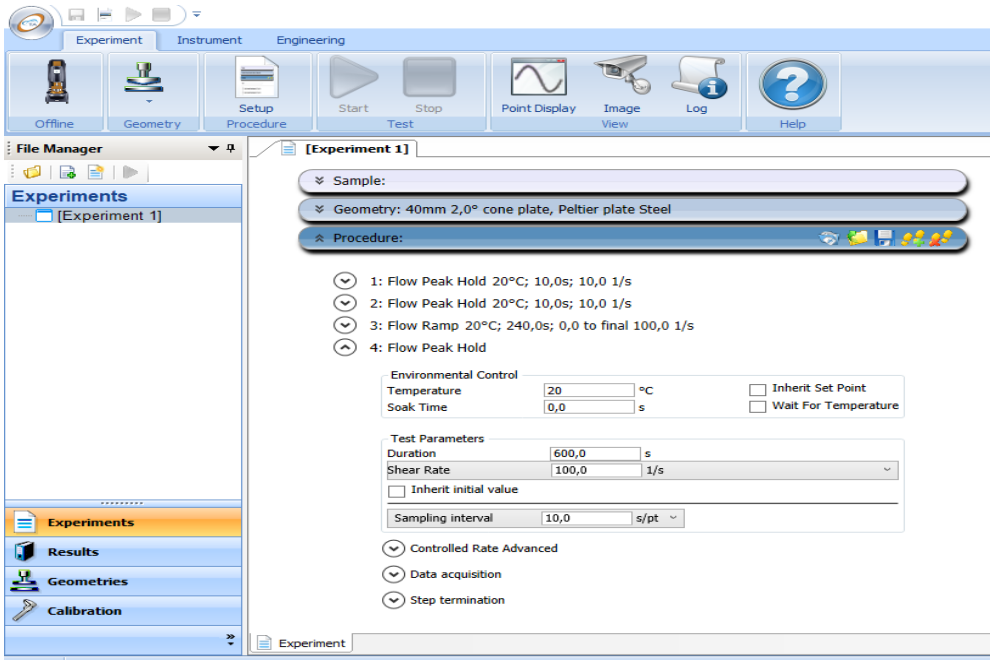

Figure III-7: Con plate geometry Peak hold 3

5. Flow ramp 2: 20℃ ;240s ; 100 to final 0 1/s :

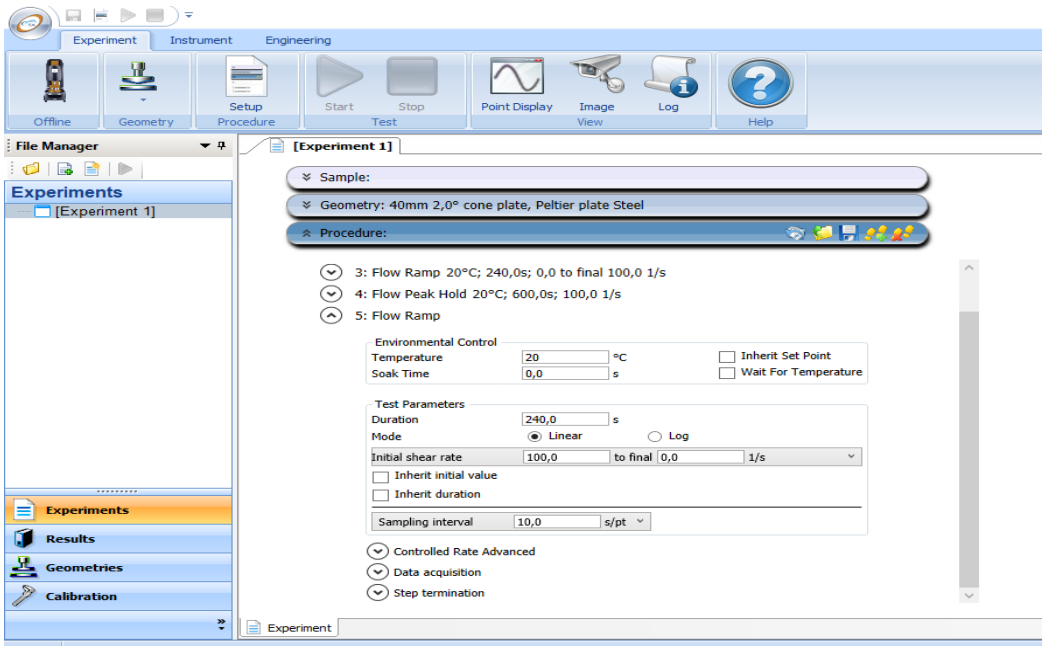

Figure III-8: Con plate geometry Flow ramp 2

III.3.2.2 Parallel plate geometry:

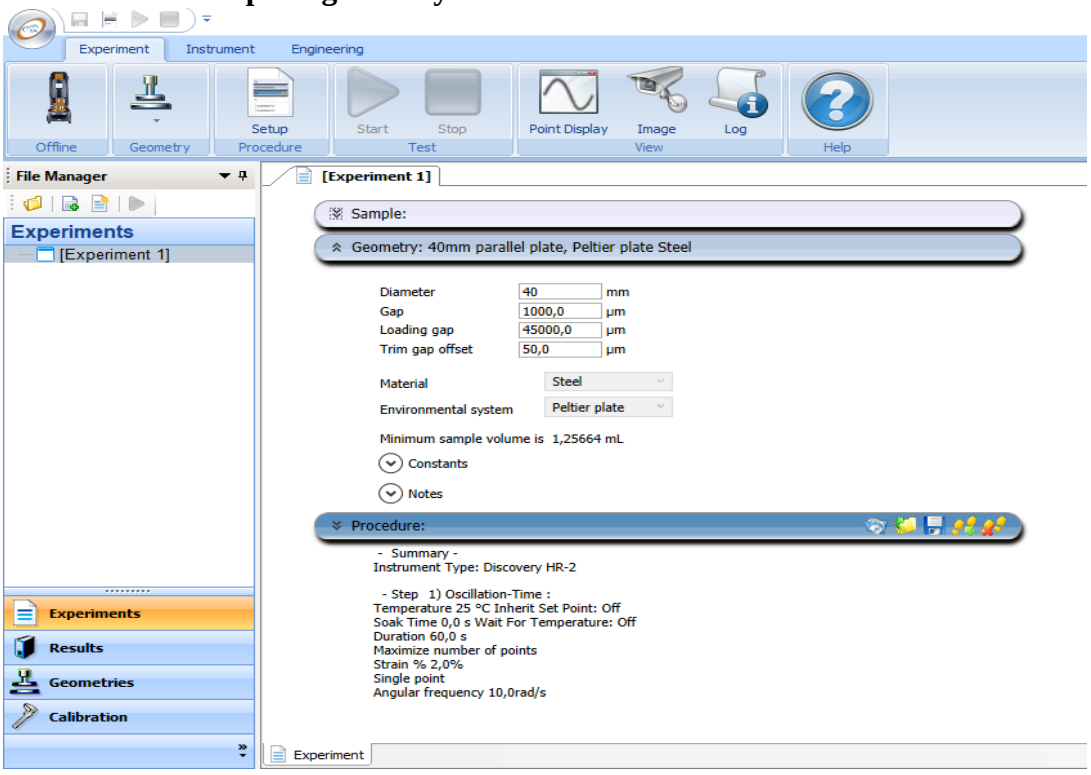

Figure III-9: Protocol 1 Parallel plate geometry dimension

1. Peak hold 1: 20°C ;10s ;10 1/s :

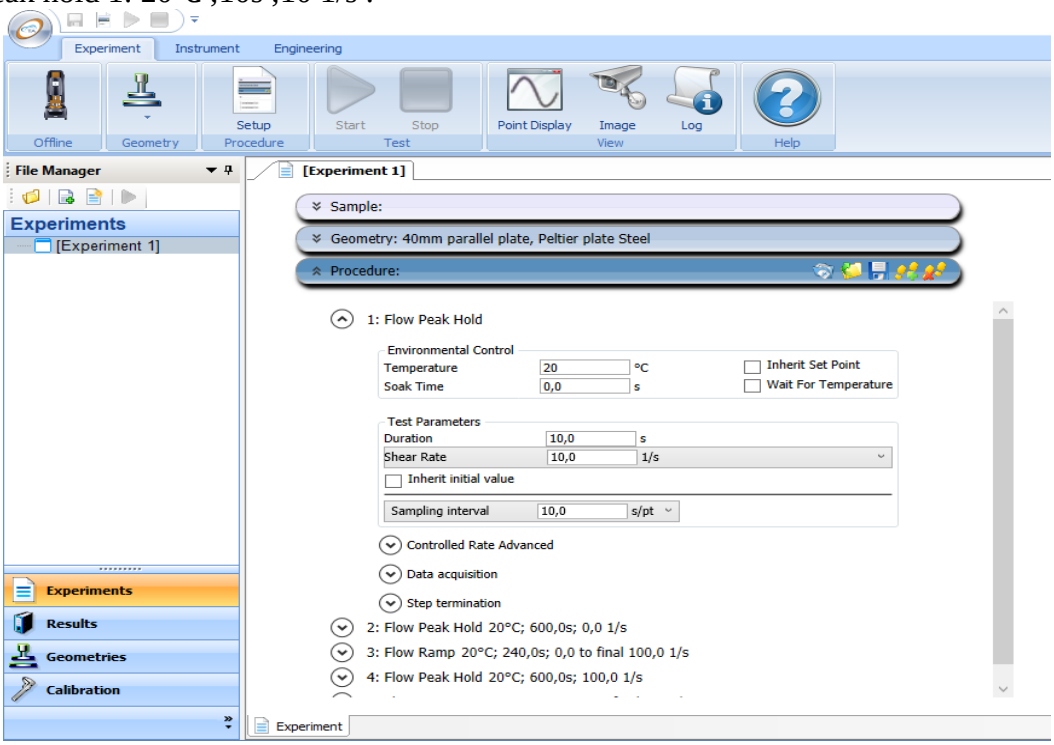

Figure III-10: Protocol 1 Parallel plate geometry Peak hold 1

2. Peak hold 2: 20°C ;600s ;0 1/s :

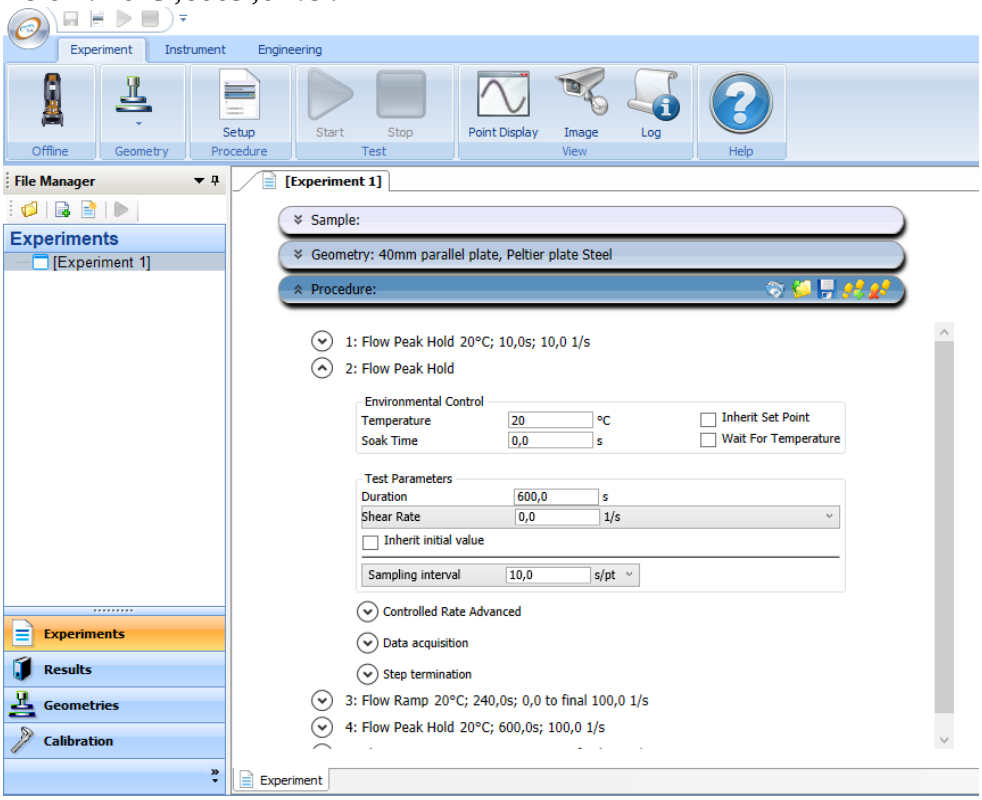

Figure III-11: Protocol 1 Parallel plate geometry Peak hold 2

3. Flow ramp 1: 20℃ 240s;0 to final 100 1/s :

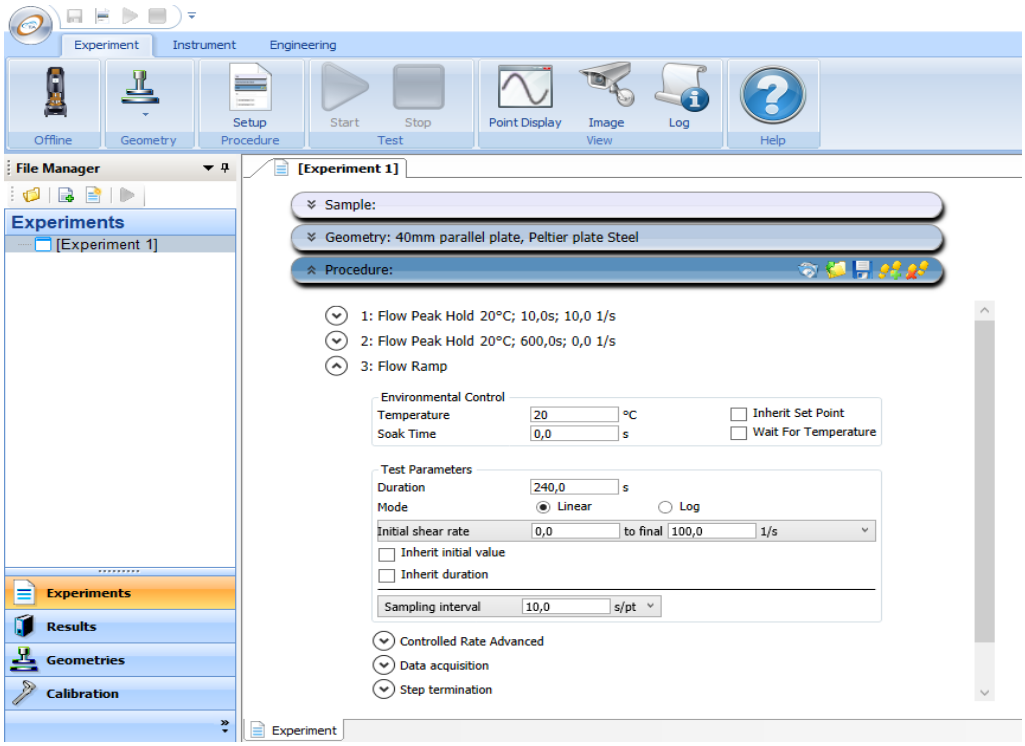

Figure III-12: Protocol 1Parallel plate geometry Flow ramp 1

4. Peak hold 3: 20℃ ;600s ;100 1/s :

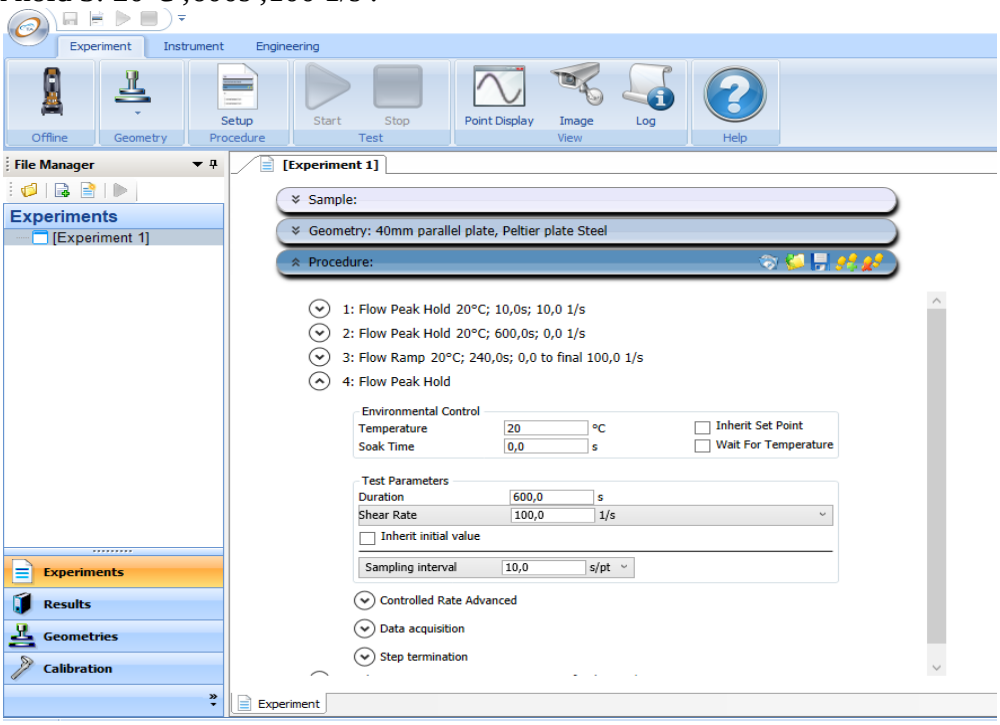

Figure III-13: Protocol 1 Parallel plate geometry Peak hold 3

5. Flow ramp 2: 20℃ ;240s ; 100 to final 0 1/s :

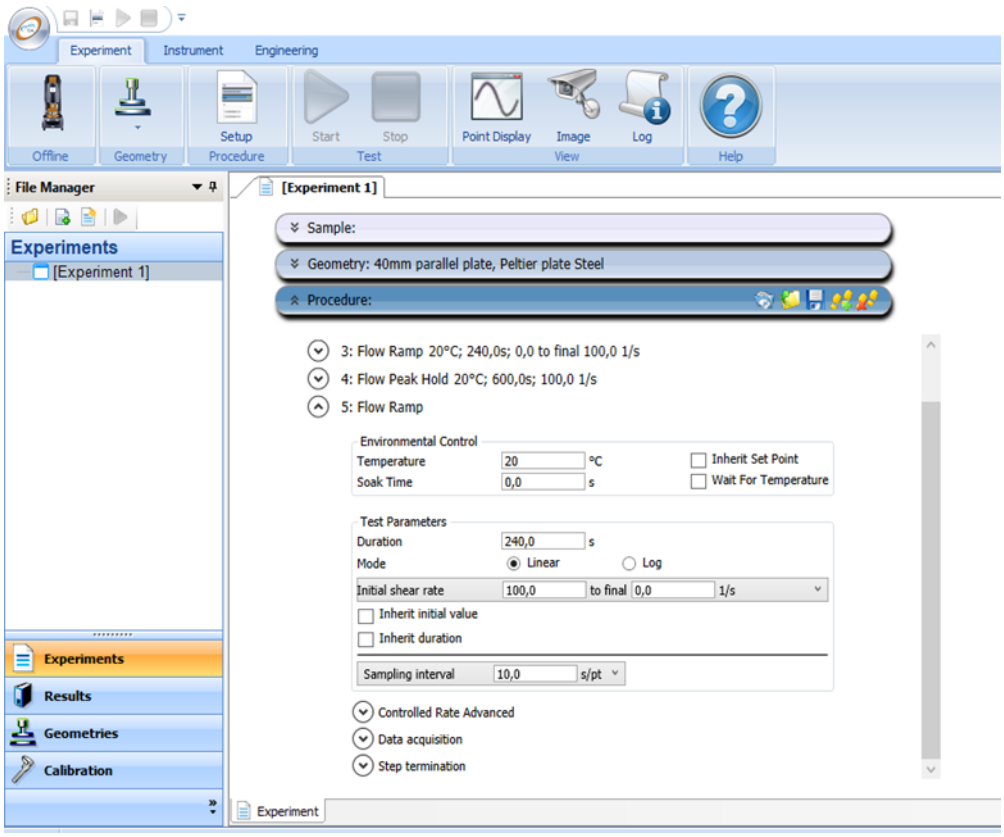

Figure III-14: Protocol 1 Parallel plate geometry Flow ramp 2

III.3.3 Protocol 2 (stress control)

III.3.3.1 Parallel plate geometry

The protocol 2 is accomplished in five steps:

To control the memory effect of the sample, we subjected the sample to a pre-shear under imposed stress (10 Pa) for 10 seconds.

Subsequently, the sample is left to rest, still under the measurement geometry, for 600 seconds. This would allow the suspension to recover, at least partially, its initial structure.

After the rest time, a succession of stress is imposed on the sample according to a rising ramp of 1800 seconds, a maximum stress level for 1800 seconds and a falling ramp of 1800 seconds.

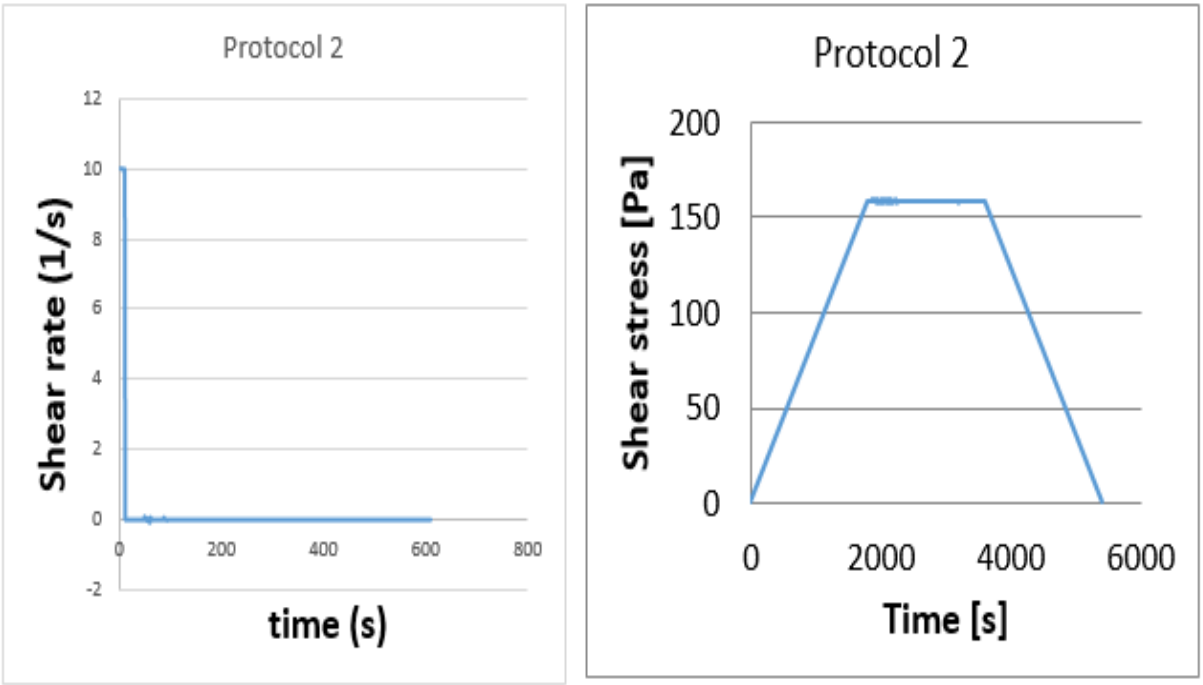

Figure III-15: Parallel plate geometry Protocol 2(stress control)

1. Peak hold 1: 20°C ;10s ;10 1/s :

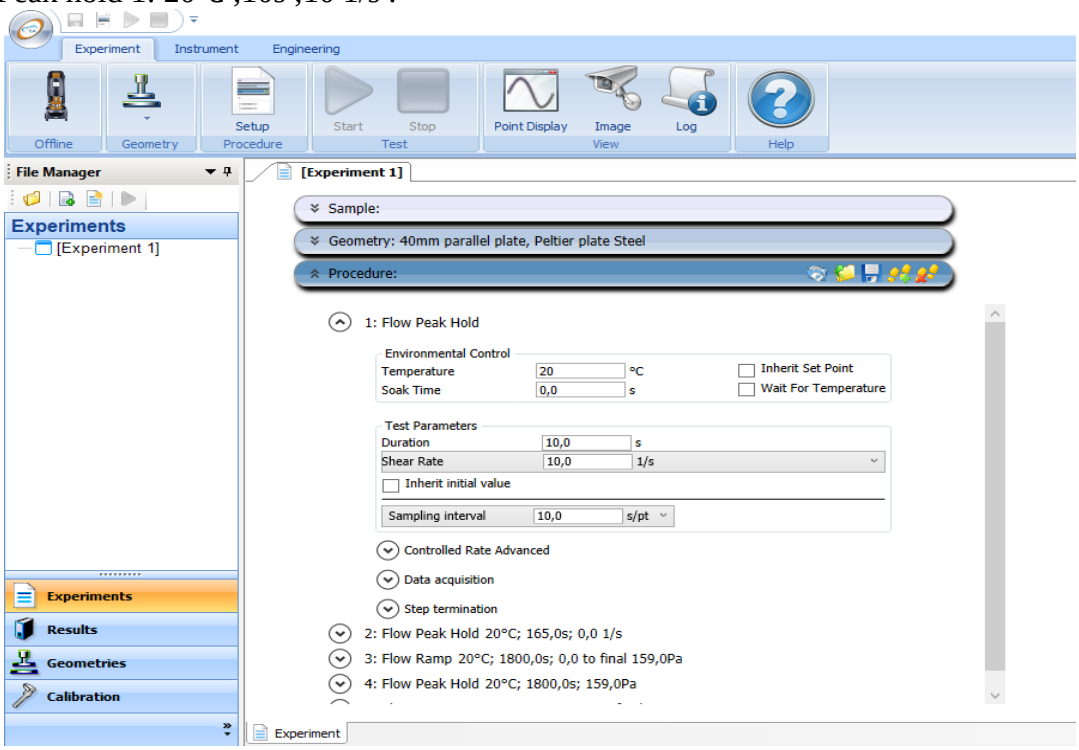

Figure III-17: Protocol 2 Parallel plate geometry Peak hold 1

2. Peak hold 2: 20°C ;600s ;0 1/s :

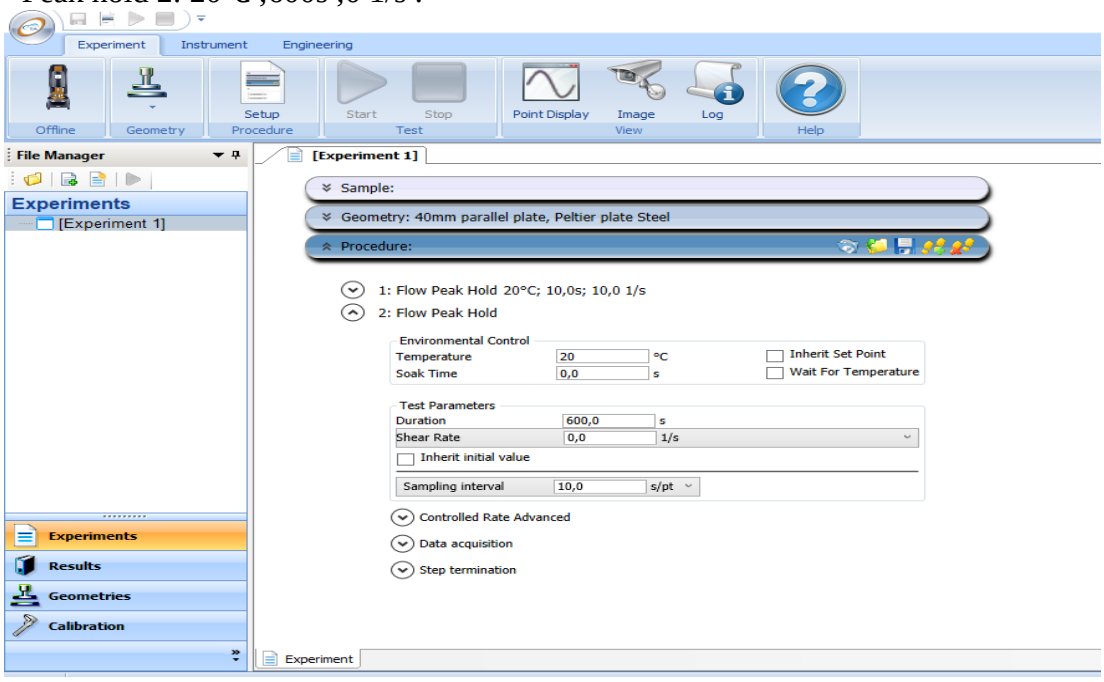

Figure III-18: Protocol 2 Parallel plate geometry Peak hold 2

3. Flow ramp 1: 20℃ 1800s;0 to final 159 pa:

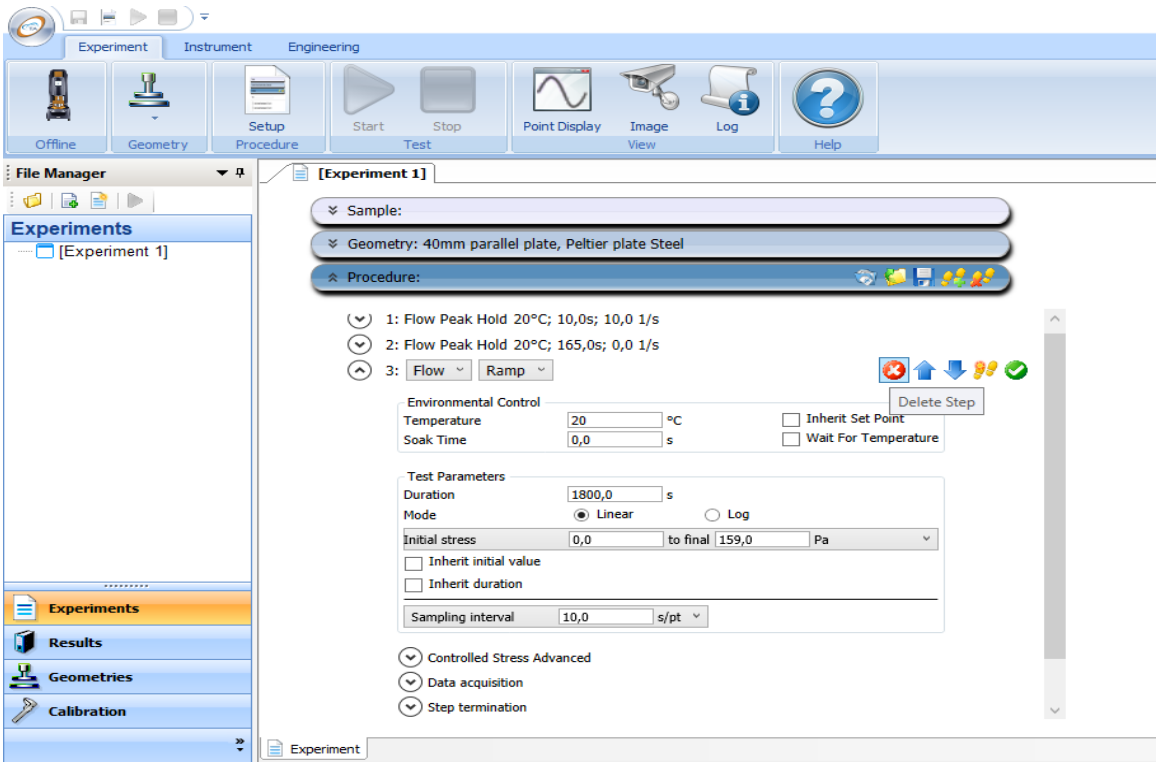

Figure III-19: Protocol 2 Parallel plate geometry Flow ramp 1

4. Peak hold 3: 20℃ ;1800s ; 159 Pa :

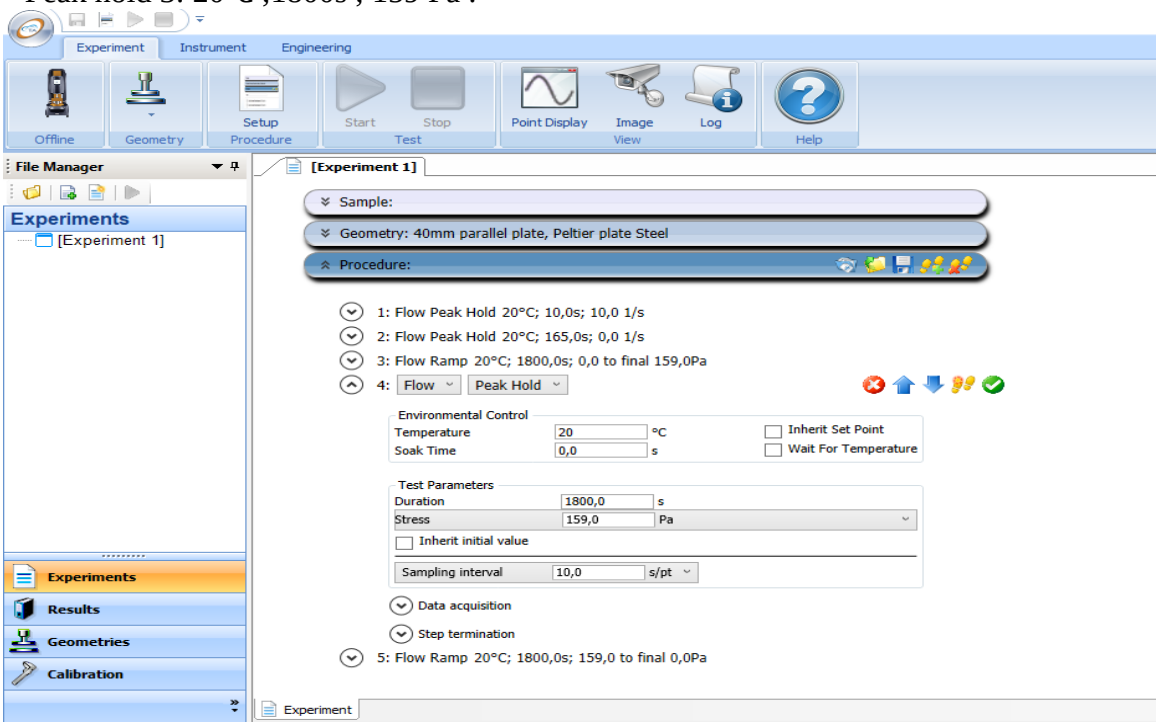

Figure III-20: Protocol 2 Parallel plate geometry Peak hold 3

5. Flow ramp 2: 20℃ ; 1800s 159 Pa to final 0 pa.

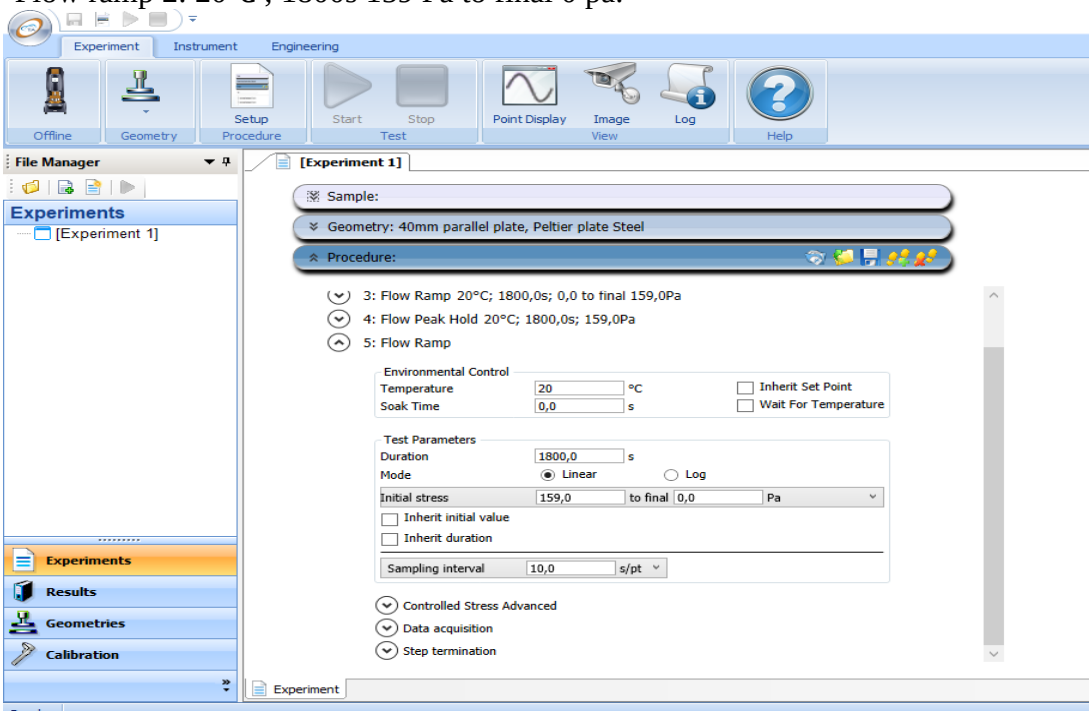

Figure III-21: Protocol 2 Parallel plate geometry Flow ramp 2

III.3.4 Calculated stress

Stress is calculated using the Herschel-Bulkley model (1926): it is described by law:

$$\tau = \tau_0 + k\dot{\gamma}^n \qquad \text{III-1}$$

Where $\tau_0$threshold constraint and k is the consistency of the fluid and n the flow index. If $n < 1$ the fluid is shear thinning and if $n > 1$ the fluid is shear thickening [7].

Chapter IV: Rheological characterization of apricot jam

IV.1 Results

IV.1.1 Protocol 1(shear rate control)

IV.1.1.1 Con plate geometry

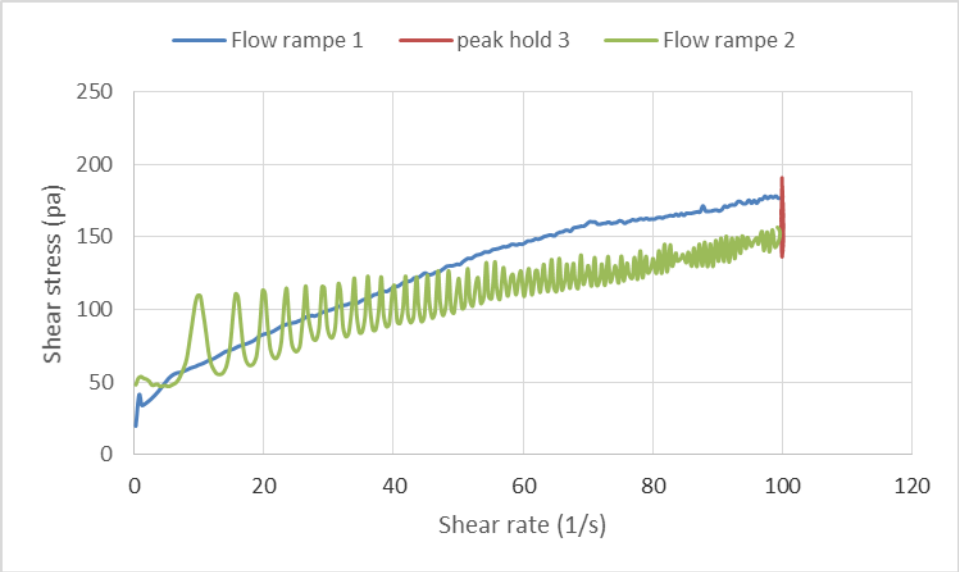

Figure IV-1: Rhéogramme of Protocol 1 con plate geometry

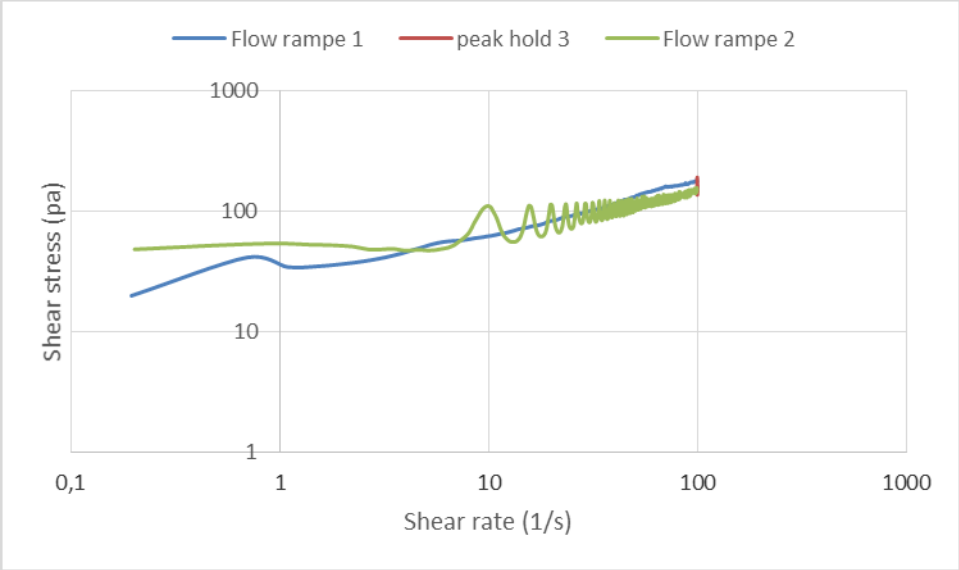

Figure IV-2: Rhéogramme of Protocol 1 con plate geometry on a logarithmic scale

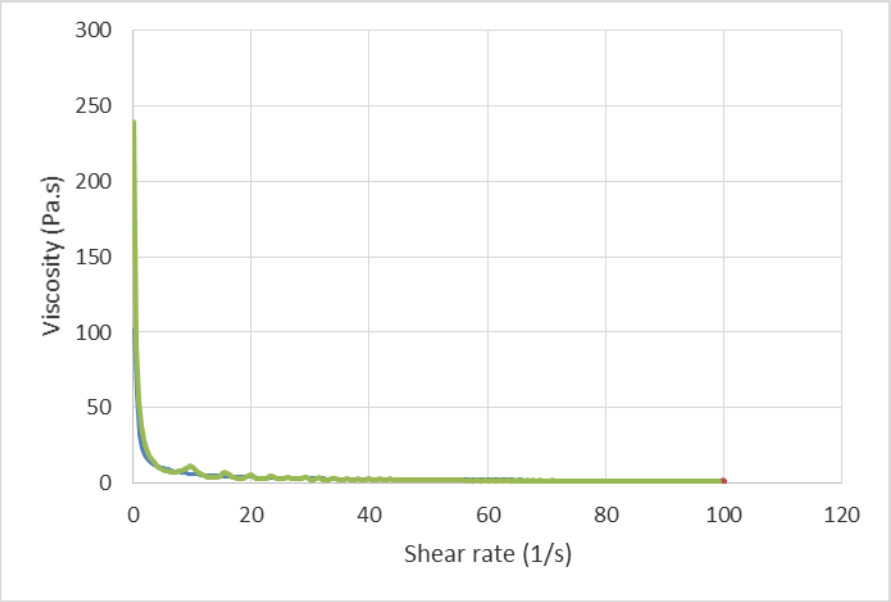

Figure IV-3: evolution of Apricot Jam viscosity in terms of shear rate in Con plate geometry

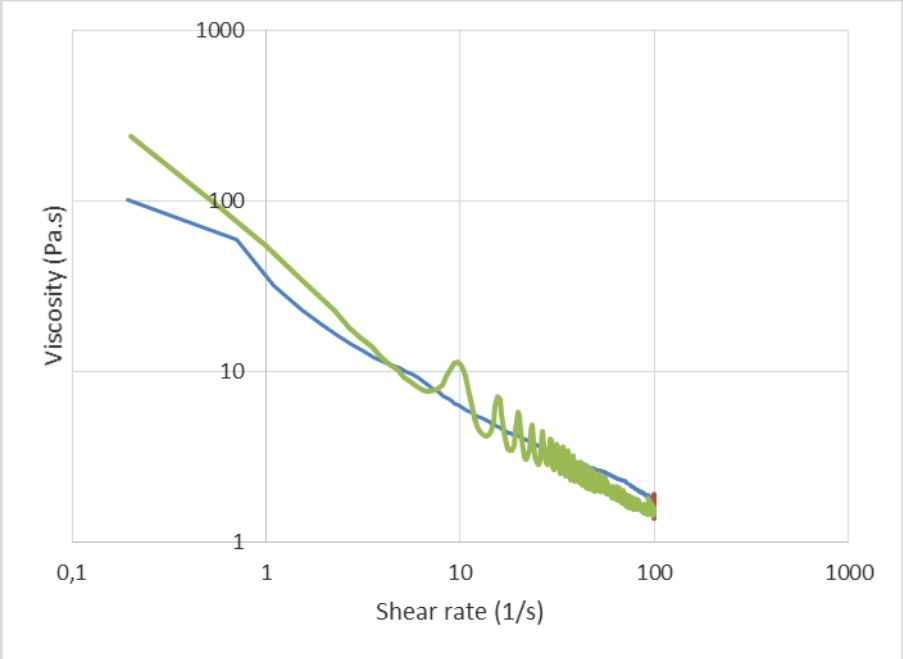

Figure IV-4: evolution of Apricot Jam viscosity in terms of shear rate in Con plate geometry on a logarithmic scale

IV.1.1.2 Parallel plate geometry

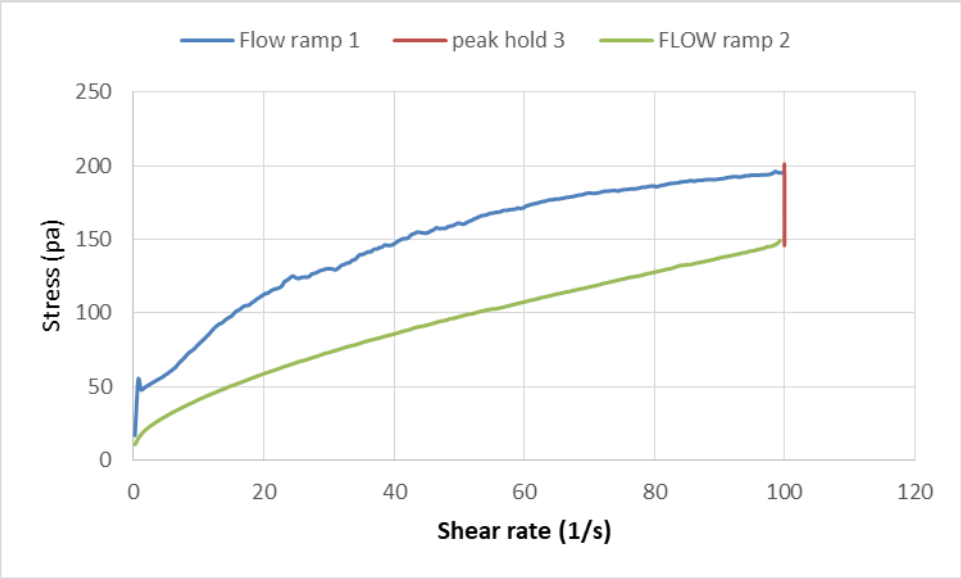

Figure IV-5: Rhéogramme of Protocol 1 (parallel plate geometry)

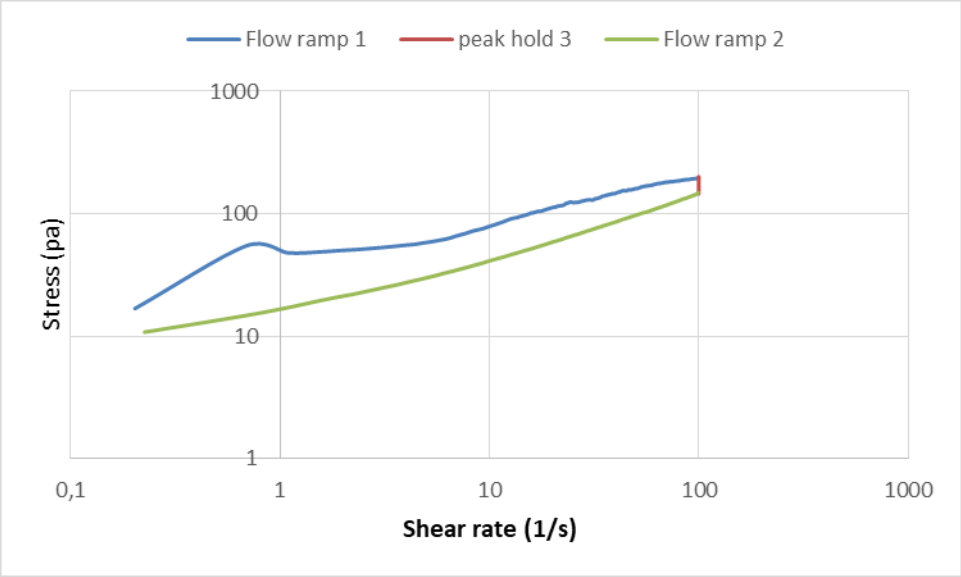

Figure IV-6: Rhéogramme of Protocol 1 (parallel plate geometry) on a logarithmic scale

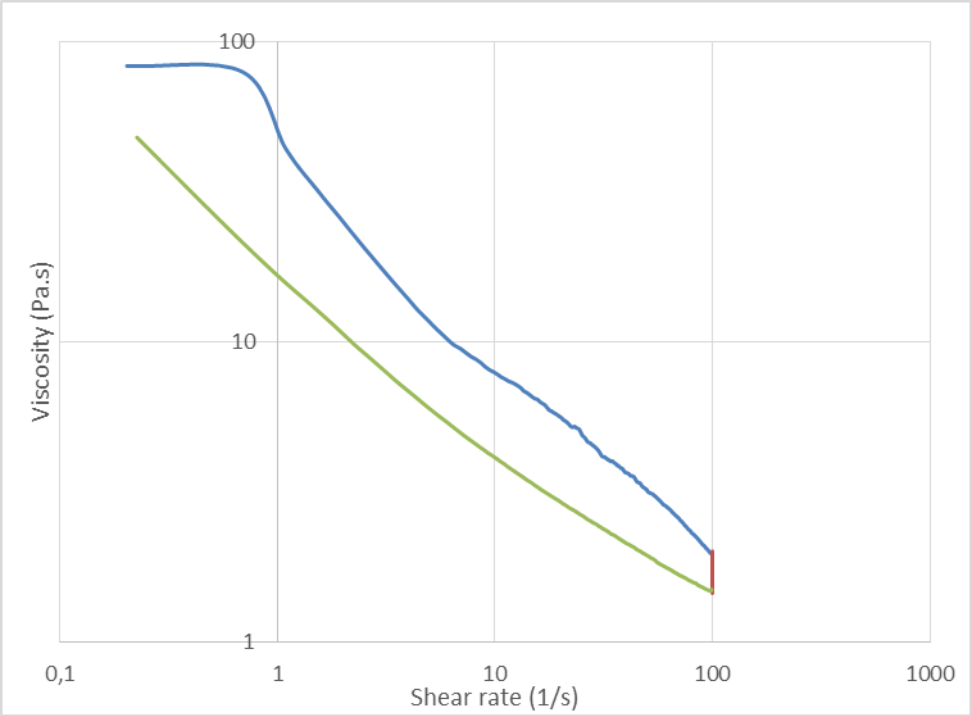

Figure IV-7: evolution of Apricot Jam viscosity in terms of shear rate in (Parallel plate geometry) on a logarithmic scale

IV.1.2 Protocol 2 (stress control)

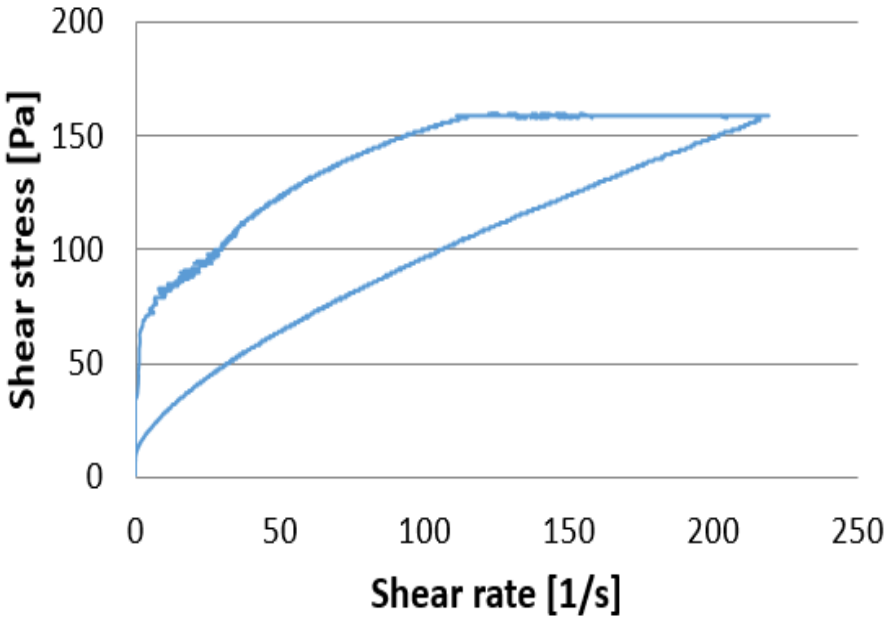

Figure IV-8: Rhéogramme of Protocol 2 (parallel plate geometry)

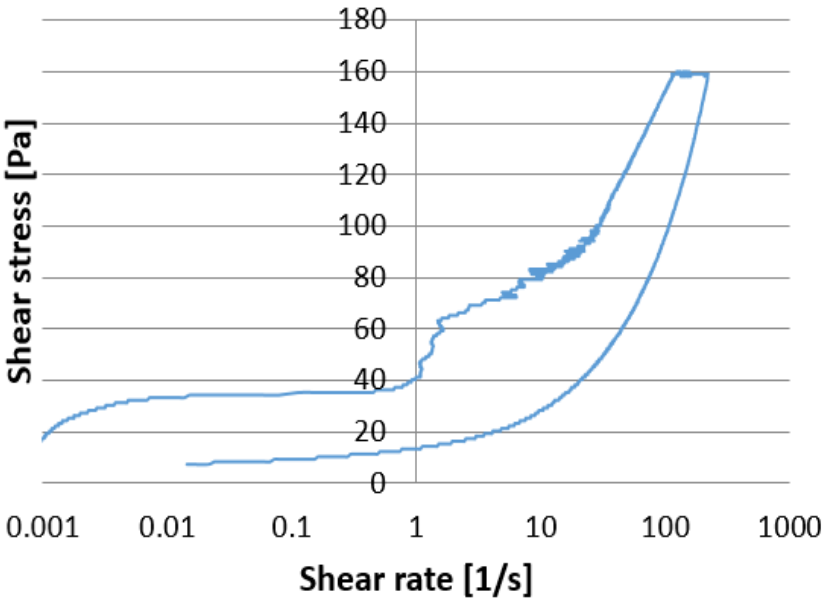

Figure IV-9: Rhéogramme of Protocol 2(parallel plate geometry) on a logarithmic scale

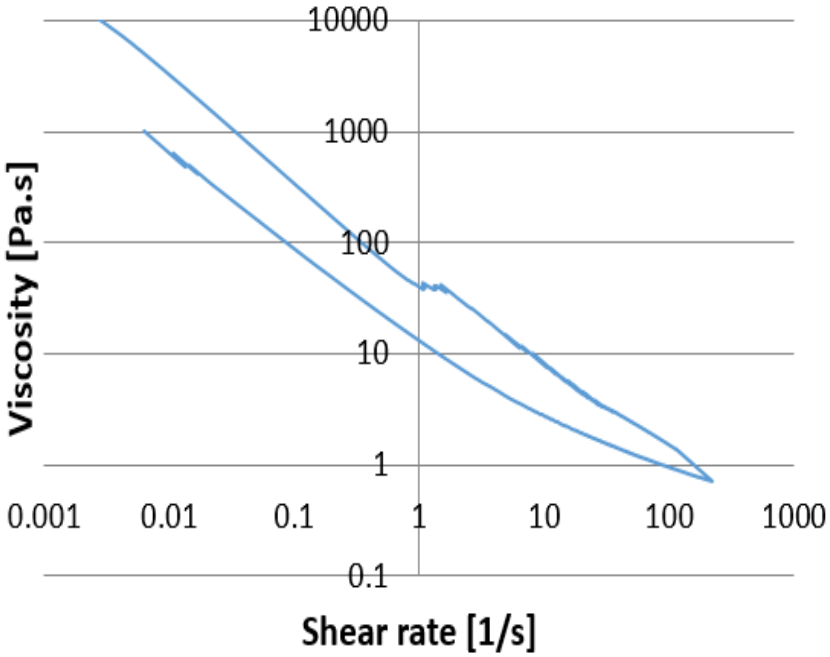

Figure IV-10: evolution of Apricot Jam viscosity in terms of shear rate in Protocol 2 (Parallel plate geometry) on a logarithmic scale

IV.2 Interpretation of the results

IV.2.1 Protocol 1

IV.2.1.1 Con plate geometry

Figure IV-1, IV-2 represent the shear stress changes in terms of the shear rate in the

Con plate geometry at constant temperature T=20℃ on a linear scale and logarithmic scale

The curves shows a non-Newtonian rheological behaviour during the flow ramp 1, while we find a deterioration in the measurement results on the flow ramp 2 and this is due to a problem in the measurement geometry, and these results are impossible to control the quality of the product.

Figure IV-3, IV- 4 represent evolution of Apricot Jam viscosity in terms of shear rate in Con plate geometry on a linear scale and logarithmic scale.

The curve on Figure IV-3 does not show accurate results due to the nature of the scale, so we plotted it on a logarithmic scale, shown in the Figure IV- 4, and we noticed a momentary decrease in the viscosity in terms of the shear rate on the flow ramp 1 and an increase in the viscosity value on the flow ramp 2.

IV.2.1.2 Parallel plate geometry

Figures Ⅳ-5, IV-6 represent the shear stress changes in terms of the shear rate in the Parallel plate geometry at constant temperature T=20℃

The curves on Figures Ⅳ-5, IV-6 show non-Newtonian rheological behaviour during the rising ramp and the falling ramp according to Herschel-Bulkley model. Through this measurement geometry, we deduce the stress value (159 pa) when the shear modulus value is 100 s^{-1}

The curve changes according to the following equation:

Flow ramp 1: $48 + 15.4748 * \dot{\gamma}^{0,50037}$

Flow ramp 2: $15 + 5,7255 * \dot{\gamma}^{0,68039}$

And the thixotropy: 58, 6 %

Figure IV- 7 represent evolution of Apricot Jam viscosity in terms of shear rate in Parallel plate geometry on a logarithmic scale

The value of viscosity gradually decreases in terms of the shear modulus until it reaches the value η = 1, 45961 Pa.s and then gradually increases until it reaches the value

η = 47, 9707 Pa.s.

IV.2.2 Protocol 2

IV.2.2.1 Parallel plate geometry

Figures Ⅳ-8, IV-9 represent the shear stress changes in terms of the shear rate in the Parallel plate geometry at constant temperature T=20℃

The curves on Figure Ⅳ-8, IV-9 show non-Newtonian rheological behaviour during the rising ramp and the falling ramp, according to Herschel-Bulkley model.

The curve changes according to the following equation:

Flow ramp 1:$35 + 16{,}023286 * \dot{\gamma}^{0{,}434727}$

Flow ramp 2: $10 + 3{,}67736 * \dot{\gamma}^{0{,}6856}$

And the thixotropie: 69, 5 %

Figure IV- 10 represent evolution of Apricot Jam viscosity in terms of shear rate in Parallel plate geometry on a logarithmic scale.

We notice a momentary change in the viscosity value, but in general it decreases gradually until it reaches the value η = 0,724163 Pa.s. And then gradually increases until it reaches the value η = 1097, 48 Pa.s.

General conclusion

The object of this study is to establish an experimental approach to quality control of the rheological behaviour of apricot jam.

First, we made a bibliographic study divided into two chapters, the first contains generalities about rheology and rotational rheometry; and the second is about the rheometer used in the experiment characterization. Then we started the experimental part, which consists of two chapters, the first is dedicated to introducing the used material and the experimental protocol; and the second chapter is devoted to the experimental results and discussions.

We conclude from the first protocol that the cone-and-plate geometry does not show good results due to the size of the aggregates in jam sample greater than the gap of the cone geometry. This made us to use plate-and-plate geometry using the first protocol in order to find the stress value corresponding to the point with a shear modulus of $100s^{-1}$, which we used in the second protocol as the maximum limit value for shear stress.

It was observed that apricot jam exhibits a time-dependent non-Newtonian behaviour which can be modelled by the Herschel-Bulkley equation; where the quality is controlled by comparing the variables τ_0 , k, and n for the samples, and the thixotropic index which calculated using the solver of MS Excel. The results were as follows:

geometry	protocol	ramp	τ_0(Pa)	k	n	Thixotropic index (%)
Parallel plate	Protocol 1	rising ramp	48	15,5	0,50	58,6
		falling ramp	15	5,7	0,68	
	Protocol 2	rising ramp	35	16,0	0,43	69,5
		falling ramp	10	3,7	0,69	

It was concluded that a simple protocol for quality control of apricot jam was proposed: subjecting the sample to a maximum stress of 159 Pa for 1800s and then subjecting it to a group of stresses on a descending flow slope for 1800s.

Abstract: Due to the lack of studies related to the rheological behaviour of local food products, in this work we study the rheological behaviour of a non-Newtonian food fluid. The aim is to proposing an experimental protocol to monitor its quality and to determine the rheological properties. We chose a local product suitable for this study which is (Omar Benomar) and used in our experiments a controlled stress rheometer (HR20). The rheological parameters and the appropriate experimental protocol, to monitor the quality of the studied apricot jam, were established. It was concluded that the Herschel-Bulkley model describes satisfactorily the rheological behaviour of the apricot jam. This rheological behaviour is quantified using the thixotropic index and the model parameters, which are: yield stress,τ_0, consistency, k, flow index, n.

Key word

Rheological behaviour, apricot jam, rheological parameters, shear stress, shear rate, viscosity.

ملخص: نظرا لقلة الدراسات المتعلقة بالسلوك الريولوجي للمنتجات الغذائية المحلية، نقوم في هذا العمل بدراسة السلوك الريولوجي لمائع لا نيوتوني غذائي بهدف اقتراح بروتوكول تجريبي لمراقبة جودته وتحديد المتغيرات الريولوجية. اخترنا منتج محلي مناسب لهذه الدراسة وهو مربى مشمش (علامة عمر بن عمر) واستعملنا في تجاربنا جهاز ريومتر(HR20). وتقترح هذه الدراسة البروتوكول التجريبي المناسب لمراقبة جودة مربى المشمش المدروس وتحديد خصائصه الريولوجية. استنتجنا أن نموذج هيرشل-بولكلي يصف بشكل مرضي السلوك الريولوجي لمربى المشمش حيث تم تقدير خصائص السلوك الريولوجي باستخدام مؤشر متغير الانسيابية وخصائص النموذج، وهي: إجهاد الحدي، τ_0، معامل التماسك، k، مؤشر التدفق ، n.

الكلمات مفتاحية

السلوك الريولوجي، مربى المشمش، الخصائص الريولوجية، إجهاد القص، معامل القص، اللزوجة

Bibliographic

[1] Malkin, Ya.A., isayev, A.," Rheology Concept, Methods, and Applications "-3rd Edition. ChemTec Publishing. 2017.

[2] Paul A. janmey, Manfred schliwa. Rheology. Current Biology Vol 18 No 15.sept ember 2008.

[3] Mezger, G. T, the rheology handbook for users of rotational and oscillatory rheometers" 4th edition." 2014, vincentz network.

[4] Mezger, G.T., the rheology handbook for users of rotational and oscillatory rheometers"2nd edition,"2006, vincentz network.

[5] Annika Björn, Paula Segura de La Monja, Anna Karlsson, Jörgen Ejlertsson and Bo H. Svensson. Rheological Characterization. Linköping University, Sweden. 20 May 2014.

[6] Benchabane, A. (2006) Etude du comportment rhéologique de mélanges argiles – polymères, Effets de l'ajout de polymères. Thèse de doctorat à l'Université Louis Pasteur – Strasbourg.

[7] Ziane Aris, (2015), Caractérisation rhéologique des polymères à basse et haute température, To obtain a master's degree in mechanical engineering, Mouloud Mammeri University of tizi ouzou.

[8] ISO, Rheology — Part 2: General principles of rotational and oscillatory rheometry. First edition.05-2021.

[9] Macosko, W.C. "Rheology Principles, Measurements and Applications". (1994).WILEY-VCH.

[10] H.A.Barnes, J.F.Hutton, Walters R.S," An introduction to rheology", (1993), Elsevier Science publishers b.v.

[11] TA Instruments, (February 2022), what are Rheometry and Rheology, https://www.tainstruments.com/what-are-rheometry-and-rheology/

[12] TA Instruments, (February 2022), Discovery hybrid rheometer, https://www.tainstruments.com/products/rheology/discovery-hybrid-rheometers/

[13] TA instruments, (2020), Rheology theory and applications, https://www .tainstruments.com/

[14] TA instruments, (February 2022), Discovery HR 20, https://www.tainstruments.com/hr-20/

[15]TA instruments, (February 2022), Discovery hybrid rheometers temperature systems and accessories, https://www.tainstruments.com/

[16] Ta instruments, (February 2022), Environmental Test Chambre, https://www .tainstruments.com/environmental-test-chamber/

[17] Ta instruments, (February 2022), Orthogonal Superposition, https://www .tainstruments.com/orthogonal-superposition/

[18] Ta instruments, (February 2022), Relative Humidity Accessory, https://www .tainstruments.com/relative- humidity-accessory/

[19] Ta instruments, (February 2022), Modular Microscope Accessory https://www .tainstruments.com/modular-microscope/

[20] Ta instruments, (February 2022), Small Angle Ligh Scattering, https://www .tainstruments.com/small-angle-light-scattering/

[21] Ta instruments, (February 2022), Electro-Rheology, https://www.tainstruments .com/electro-rheology/

[22] Ta instruments, (February 2022), Starch Pasting Cell, https://www.tainstruments.com/starch-pasting-cell/

[23]Ta instruments, ((February 2022), Interfacial Rheology, https: //www.tainstruments. com/interfacial-accessories/

[24] Ta instruments, (February 2022), Inter facial Exchange Cell,https://www .tainstruments.com/interfacial-exchange-cell/

[25] Ta instruments, (February 2022), Optical Plate Accessory (OPA), http://www .tainstruments.com/optical-plate/

[26] Ta instruments,(February 2022), UV Curing Accessories, https://www.tainstruments. com/uv-curing-accessories/

[27] Ta instruments, (February 2022), Dielectric Measurement, https://www .tainstruments.com/dielectric-measurement/.

[28] Ta instruments, (February 2022),, Immobilization Cell, https://www.tainstruments. com/immobilizatio-n-cell/

[29] Ta instruments, (February 2022), Tribo-Rheometry, https://www.tainstruments. com/tribo-rheometry-accessory/

[30] Touati, N., Tarazona-Diaz M.P, Aguayo, Encarna., Louaileche H., Effect of storage time and temperature on the physicochemical and sensory characteristics of commercial apricot jam. Food Chemistry. 27-23-2014

[31] Food and Agriculture Organization of the United Nations, 1995, JAM, https://www.fao.org/home/en

[32] Ann E. Henderson, Charlotte Brennand, Apricots, March 2010, Utah State University

[33] Susan Azam Ali, "Home-based fruit and vegetable processing", 2008, Food and Agriculture Organization of the United Nations.

[34] Food and Agriculture Organization of the United Nations, world health organization. 2016, Pectins. https://www.fao.org/home/en, https://www.who.int/ar.

[35] Catherine Renard, Jean François Maingonnat. Thermal Processing of Fruits and Fruit Juices. HAL. 5 Jun 2020

[36] Charlotte P, Brennand, "Home Drying of Food".Utah State University Extension. August 1994.

[37] Towseef A. Wani, Quraazah A. Amin , S. Fauzia , N. Dorjey , B.A. Zargar , Phuntsog Tundup , Kunzanglamo1 , N. Deldan , R. Safal1 and M.A. Beigh**.** Standardization, Stability Study and Chemical Properties of Apricot Jam Prepared in Cold Arid Region of Ladakh. International Journal of Current Microbiology and Applied Sciences.2019. http://www.ijcmas.com

[38] Eatbydate, (April 2015), How Long Does Jam/Jelly Last, http://www .eatbydate.com/other/condiments/how-long-does-jam-last-shelf-life-expiration-date/